Inorganic Chemistry
Cite This: Inorg. Chem. XXXX, XXX, XXX−XXX
Article
pubs.acs.org/IC

Converging Energy Transfer in Polynuclear Ru(II) Multiterpyridine Complexes: Significant Enhancement of Luminescent Properties

Simon Cerfontaine,[†] Lionel Marcélis,[†] Baptiste Laramee-Milette,[‡] Garry S. Hanan,[‡] Frédérique Loiseau,[§] Julien De Winter,[∥] Pascal Gerbaux,[∥] and Benjamin Elias*[,†]

[†]Institut de la Matière Condensée et des Nanosciences (IMCN) − Molécules, Solides et Réactivité (MOST), Université catholique de Louvain, Place Louis Pasteur 1, bte L4.01.02, B-1348 Louvain-la-Neuve, Belgium

[‡]Département de Chimie, Université de Montréal 2900 Edouard-Montpetit, Montréal, Québec H3T-1J4, Canada

[§]Département de Chimie Moléculaire, Université Grenoble-Alpes, CNRS UMR 5250, BP53 38041 Grenoble, France

[∥]Organic Synthesis and Mass Spectrometry Laboratory, University of Mons − UMons, 23 Place du Parc, B-7000 Mons, Belgium

Supporting Information

ABSTRACT: Ruthenium-based complexes are widely used as photocatalysts, as photosensitizers, or as building blocks for supramolecular assemblies. In the field of solar energy conversion, building light harvesting antenna is of prime interest. Nevertheless, collecting light is mandatory but not sufficient; once collected and transferred, the exciton has to be long-lived enough to be transferred to a catalytic site. If Ru(II) terpyridine complexes are prime building blocks for structural reasons, the short lifetime of their excited state prevents their use as a harvesting center in light antennae. In this paper, we present new polynuclear assemblies, based on Ru(II)-terpyridine units where delocalization of the excited state is combined with an antenna effect. As a consequence, complexes **C1**−**C3** display long-lived excited states compared to $[Ru(tpy)_2]^{2+}$, making them promising efficient antenna building blocks to be connected to a final acceptor or a catalytic center.

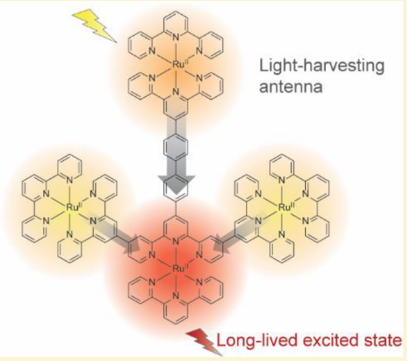

INTRODUCTION

The synthesis of the complexes $[Ru(tpy)_2]^{2+}$ (tpy or terpyridine = 2,2′:6′,2″-terpyridine)[1] and $[Ru(bpy)_3]^{2+}$ (bpy = 2,2′-bipyridine)[2] in the midthirties and the first reports on their photophysical properties[3,4] have led to considerable research over the past decades on Ru(II) polypyridyl-based complexes.[5−9] Due to their electrochemical and photophysical properties, Ru(II) polypyridyl complexes are first-class building blocks in the field of photo- and supramolecular chemistry.[5,6,10] Among other applications, their use in light-harvesting antennae has been nicely shown in the literature by several groups.[11−14] When building multinuclear assemblies, bis-tridentate Ru(II) complexes are more suitable compared to tris-bidentates, because the former ones do not show the occurrence of stereoisomers, and thus they allow well-designed and defined geometric patterns.[5] However, bis-terpyridine Ru(II) complexes are almost nonemissive under normal conditions and have poor excited-state properties due to the close proximity of the ^{3}MLCT (metal-to-ligand charge-transfer) state and the ^{3}MC (metal-centered) state. Nevertheless, this drawback may be partially overcome by an adequate design of the ligands and the complexes.[7,15] Several strategies have been developed to stabilize the ^{3}MLCT state or to destabilize the ^{3}MC state, thereby increasing the ^{3}MLCT-^{3}MC energy gap. Among the most promising approaches are the reduction of the angular strain around the metal center,[16−20] the incorporation of strong σ-donor moieties onto the ligands,[21−27] and the lowering of the LUMO level.[27−31] In all cases, significant modification of the terpyridine ligand is required to achieve increase in excited-state lifetime and quantum yields. In the present work, the simple grafting of whole terpyridines one to another leads to significant increases in both luminescence quantum yield and excited-state lifetime. The robustness of the bis-tridendate ruthenium(II) complexes allows the synthesis of Ru(II) multinuclear complexes[5,32−44] enabled by the use of ligands with multiple terpyridine binding sites. As shown in the literature, only multinuclear complexes[32,34,35,37,40−44] with more than two Ru(II) centers are promising candidates for the formation of dendrimers and light harvesting systems.

Previously in our laboratory, we reported the synthesis of new polyterpyridine ligands;[45] these three ligands, **L1**−**L3**, depicted in Scheme 1, are characterized by the presence of nonequivalent terpyridine sites, since a *central* terpyridine unit, the three pyridine cycles of which are substituted, is used to connect *lateral* terpyridine moieties which are only derivatized on the 4′ position. These ligands possess thus nonequivalent chelation sites, which could influence the properties of the resulting metallic assembly. Indeed, the presence of non-equivalent metal centers could enable energy transfer between these sites, allowing the development of molecular antenna for example. In the aim to study the influence of the *central*

Received: December 1, 2017

DOI: 10.1021/acs.inorgchem.7b03040
Inorg. Chem. XXXX, XXX, XXX−XXX

Scheme 1. Synthetic Scheme for Complexes C1 to C5[a]

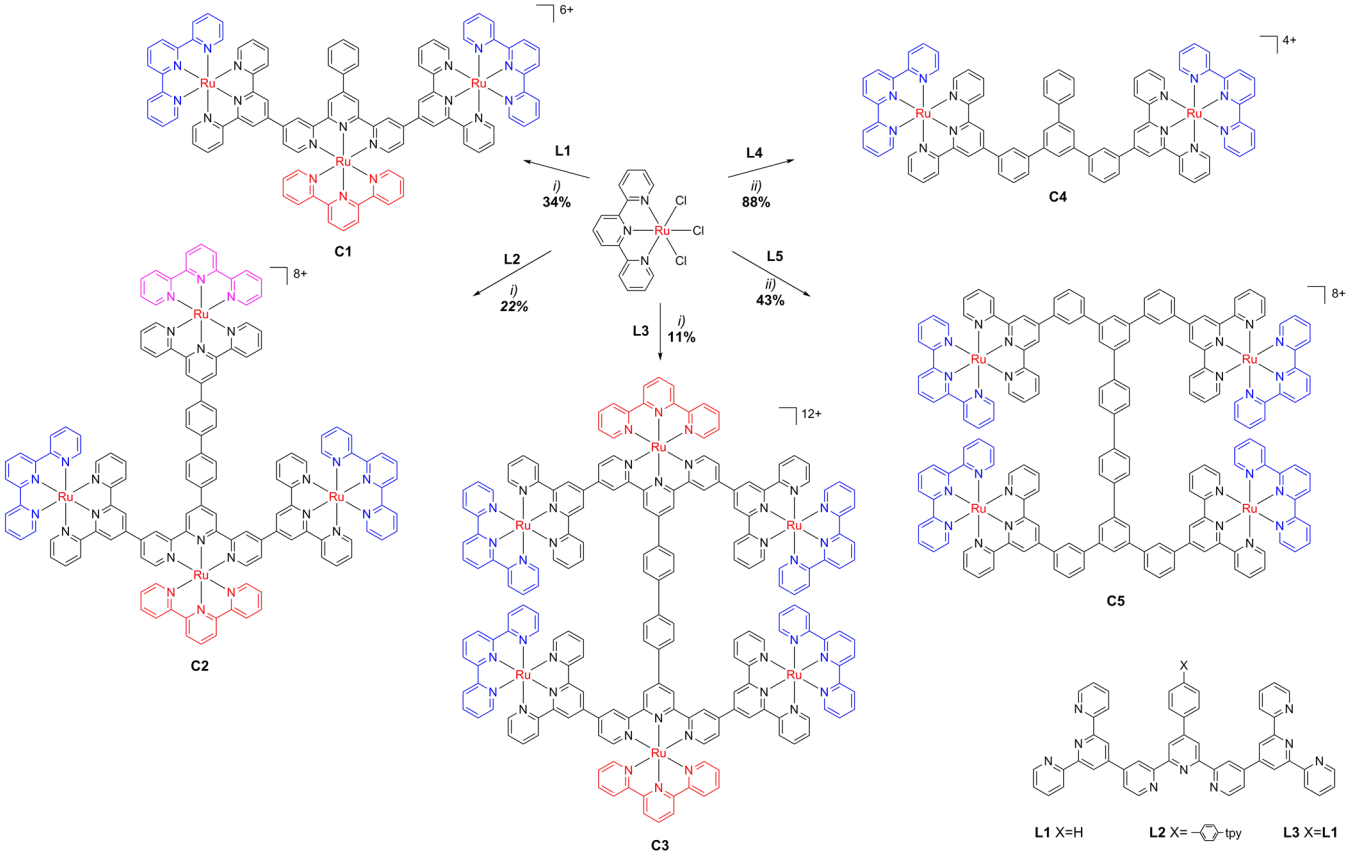

[a]Reaction conditions: (i) *N*-ethylmorpholine, H_2O/isopropanol (1/1), reflux, 3 days, (ii) *N*-ethylmorpholine, H_2O/isopropanol/HFIP (4/3/1), reflux, 3 days.

terpyridine chelation site, two new ligand analogs were synthesized (**L4**–**L5**, Scheme 2); these ligands do not possess the *central* terpyridine binding site.

In this paper, five new multinuclear complexes, depicted in Scheme 1, were synthesized and characterized by NMR spectroscopy, high resolution mass spectrometry, cyclic voltammetry, and absorption and emission spectroscopy. Three of the new complexes synthesized showed convergent energy transfer from the *peripheral* Ru(II) centers to the *central* Ru(II) moiety.

EXPERIMENTAL SECTION

Materials and Instrumentation. All solvents and reagents for the synthesis are of reagent grade and are used without any further purification. All solvents for the spectroscopic and electrochemical measurements are of spectroscopic grade. 2,2′:6′,2″-terpyridine (Alpha Aesar), $RuCl_3.xH_2O$ (Acros), 1,3,5-tribromobenzene (Acros), 4,4′-dibromodiphenyl (Acros), N-ethylmorpholine (Acros), ammonium hexafluorophosphate (Fluorochem), $Pd(PPh_3)_2Cl_2$ (Acros), Na_2CO_3 (Acros), $Pd(dppf)Cl_2$ (Fluorochem), Bis(pinacolato)diboron (Fluorochem), hexafluoroisopropanol (Fluorochem), K_2CO_3 (Acros), KNO_3 (Acros), *t*-BuOH (Acros), Al_2O_3 neutral (Acros), SiO_2 (Rocc). 3,5-dibromo-1,1′-biphenyl[46] and (3-([2,2′:6′,2″-terpyridin]-4′-yl)phenyl)boronic acid[47] were synthesized as previously reported. Water is purified with a Millipore Milli-Q system. For the Ru(II) complexes the reaction mixtures were degassed by bubbling argon during 15 min. The precipitates were isolated by spinning at 6000 rpm for 5 min in a Hettich Universal 320 centrifuge. NMR experiments were performed in $CDCl_3$ or CD_3CN on a Bruker AC-300 Avance II (300 MHz) or on a Bruker AM-500 (500 MHz) at 20 °C. The chemical shifts (given in ppm) are measured vs the residual peak of the solvent as the internal standard. UV–vis absorption spectra were recorded on a Shimadzu UV-1700. Fluorescence spectra were recorded on a FluoroLog3 FL3–22 from Jobin Yvon equipped with an 18 V, 450 W xenon short arc lamp and an R928P photomultiplier, excitation and emission spectra are corrected for the instrument response. Luminescence lifetime measurements were performed after irradiation at λ = 400 nm obtained by the second harmonic of a Titanium:Sapphire laser (picosecond Tsunami laser spectra physics 3950-M1BB+39868–03 pulse picker doubler) at a 80 kHz repetition rate. The Fluotime 200 from AMS technologies was used for the decay acquisition. It consists of a GaAs microchannel plate photomultiplier tube (Hamamatsu model R3809U-50) followed by a time-correlated single photon counting system from Picoquant (PicoHarp300). The ultimate time resolution of the system is close to 30 ps. Luminescence decays were analyzed with FLUOFIT software available from Picoquant. Transient absorption spectra were acquired using a LP920 K system from Edinburgh Instruments. Excitation was carried out from the third-harmonic (355 nm) of a Brillant-Quantel Nd:YAG laser at 6 Hz. A Xe900 pulsed Xenon Lamp is used as probe source. The photons were dispersed using a monochromator, transcripted by a R928 (Hamamatsu) photomultiplicator and recorded on a TDS3012C (Tectronix) oscilloscope. Combination of this equipment with an Oxford Instrument Optistat DN cryostat was used for the luminescent lifetime as a function of the temperature. Cyclic voltammetry was carried out in a one-compartment cell, using a glassy carbon disk working electrode (approximate area = 0.03 cm^2), a platinum wire counter electrode, and an Ag/AgCl reference electrode. The potential of the working electrode was controlled by an Autolab PGSTAT 100 potentiostat through a PC interface. The cyclic voltammograms were recorded with a sweep rate of 100 mV s^{-1}, in dried acetonitrile or N,N-dimethylformamide (Sigma-Aldrich, HPLC grade). The concentration

DOI: 10.1021/acs.inorgchem.7b03040
Inorg. Chem. XXXX, XXX, XXX–XXX

Scheme 2. Synthetic Schemes (a) for the Ligand L4 and (b) for the Ligand L5[a]

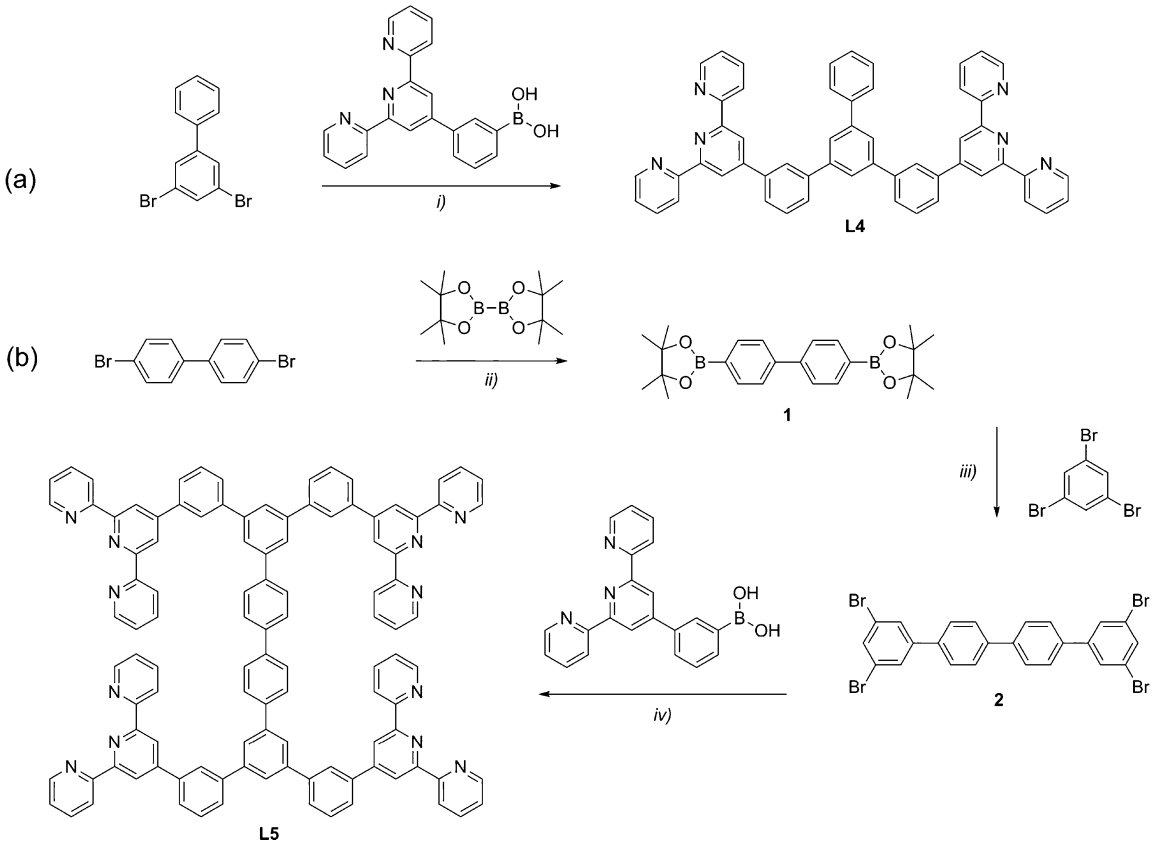

[a]Reaction conditions: (i) $[Pd(PPh_3)_2Cl_2]$, Na_2CO_3, Toluene/t-BuOH/H_2O (9/2/10), 110°C, 3 days, 80%; (ii) $[Pd(dppf)Cl_2]$, KOAc, DMSO, 80 °C, 10 h, 93%; (iii) $[Pd(PPh_3)_2Cl_2]$, toluene/K_2CO_3 2 M (2/1), 100 °C, 18 h, 36%; (iv) $[Pd(PPh_3)_2Cl_2]$, Na_2CO_3, Toluene/t-BuOH/H_2O (15/2/3), 110 °C, 3 days, 19%.

of the complexes was 8×10^{-4} mol L^{-1}, with 0.1 mol L^{-1} tetrabutylammonium perchlorate as supporting electrolyte. Before each measurement, the samples were purged by nitrogen. For organic compounds, APCI mass spectra were recorded by using a Q-Extractive orbitrap from ThermoFisher and EI mass spectra were recorded using a TSQ7000 from Finnigan. For complexes: Matrix Assisted Laser Desorption/Ionization Time-of-Flight (MALDI-ToF) mass spectra were recorded using a Waters QToF Premier mass spectrometer equipped with a Nd:YAG laser using the third harmonic with a wavelength of 355 nm. In the context of this study, a maximum output of ~65 J is delivered to the sample in 2.2 ns pulses at 50 Hz repeating rate. Time-of-flight mass analyses were performed in the reflection mode. The matrix, trans-2-[3-(4-*tert*-butyl-phenyl)-2-methyl-2-propenylidene]malononitrile (DCTB), was prepared as a 40 mg/mL solution in chloroform. The matrix solution (1 μL) was applied to a stainless steel MALDI target and air-dried. Samples were dissolved in acetonitrile to obtain 1 mg/mL solutions. Then, 1 μL aliquots of these solutions were applied onto the target area (already bearing the matrix crystals) and then air-dried. High resolution ESI mass spectra were recorded using Waters Synapt G2-Si mass spectrometer. The solution (~10^{-6} mol L^{-1} in acetonitrile) is directly infused in the ESI source with a typical flow rate of 5 μL min^{-1} with a capillary voltage of 3.1 kV, a source temperature of 100 °C and a desolvation temperature of 200 °C. The quadrupole was set to pass ions from 100 to 2000 Th and all ions were transmitted into the pusher region of the time-of-flight analyzer (Resolution ~20,000) for mass-analysis with 1 s integration time. Data were acquired in continuum mode until acceptable average data were obtained.

Franck–Condon Analyses for Emission Spectra. Fitting of the steady-state photoluminescence spectra at 77K was made possible through Franck–Condon line-shape analysis. After converting the wavelength abscissa values to energy, the emission spectral data (multiplied by λ^2) are renormalized and fitted using eq 1 corresponding to Franck–Condon line-shape prediction taking into account two vibration modes.

$$I(\tilde{\nu}) = \sum_{\nu_m=0}^{\infty}\sum_{l=0}^{\infty}\left[\left(\frac{E_{00} - \nu_m\hbar\omega_m - \nu_l\hbar\omega_l}{E_{00}}\right)^4 \frac{S_M^{\nu_m}}{\nu_m!} \frac{S_L^{\nu_n}}{\nu_l!} \exp\left\{-4\ln 2\left[\frac{\tilde{\nu} - E_{00} + \nu_m\hbar\omega_m + \nu_l\hbar\omega_l}{\Delta\tilde{\nu}_{1/2}}\right]^2\right\}\right] \quad (1)$$

In this equation, ν_m and ν_l are the vibrational quantum numbers for the acceptor mode, S_M and S_L are the Huang–Rhys factor, also known as the coupling factor, $\hbar\omega_m$ and $\hbar\omega_l$ correspond to the vibrational energy spacing in the ground-state potential energy surface for the corresponding vibration mode, E_{00} corresponds to the energy difference between the ground and excited-state potential surfaces. Luminescence spectra can be modeled using one or two vibration modes, which correspond to the dominant vibration mode or an average of vibration. Usually, transitions implying $\nu^* = 0$ to $\nu = 0$ to 5 are sufficient to fit the experimental data. These transitions are broadened thanks to a Gaussian distribution to take into account solvent effects; $\Delta\nu_{1/2}$ is the full-width at half-maximum of the broadening for the transition and a normalization factor of 4 ln 2 is added to ensure that the integrated area corresponds to the intensity of the line that is broadened into a Gaussian distribution.

Theoretical Calculations. All calculations were performed with the Gaussian09,[48] revision E.0 suite of programs employing the DFT method, the Becke three-parameter hybrid functional, and Lee–Yang–Parr's gradient-corrected correlation functional (B3LYP).[49−51] All

DOI: 10.1021/acs.inorgchem.7b03040
Inorg. Chem. XXXX, XXX, XXX−XXX

elements except ruthenium were assigned the 6-31G*(d,p) basis set. The double- ζ quality SBKJC VDZ ECP basis set with an effective core potential was employed for the Ru ion.[52−55] No imaginary frequencies were obtained when frequency calculations on optimized geometries were performed. GaussView 5.0.9,[56] GaussSum 3.0[57] and Chemissian 4.30[58] software were used for data analysis, visualization and surface plots. All calculations were performed in a MeCN solution by using the polarized continuum solvation model, as implemented in Gaussian 09.[59,60]

Synthesis and Characterization. *4′,4′′′′-(5′-Phenyl-[1,1′:3′,1″-terphenyl]-3,3″-diyl)di-2,2′:6′,2″-terpyridine (L4).* To a mixture of 3,5-dibromo-1,1′-biphenyl (0.1000 g, 0.3204 mmol, 1 equiv), (3-([2,2′:6′,2″-terpyridin]-4′-yl)phenyl)boronic acid (0.3395 g, 0.9612 mmol, 3 equiv) and Na_2CO_3 (0.2038 g, 1.9224 mmol, 6 equiv) was added a solution of water/tert-butanol/toluene (42 mL, 10/2/9). The reaction mixture was degassed by four freeze−pump−thaw cycles; after the third cycle; when the reaction mixture was frozen the $[Pd(PPh_3)_2Cl_2]$ (0.0225 g, 0.0320 mmol, 0.1 equiv) was added and one more freeze−pump−thaw cycles was done. The reaction mixture was heated to 110 °C during 3 days under argon atmosphere. 100 mL of water was added to the reaction mixture and the aqueous phase was extracted three times with 150 mL CH_2Cl_2. Organic layers were combined, dried over $MgSO_4$ and solvents were then removed under vacuum. The off-white powder was purified by column chromatography on neutral Al_2O_3 (CH_2Cl_2/MeOH: 98/2) and washed one time with MeOH to afford **L4** (0.1971 g, 80%) as a white powder. ^{1}H NMR ($CDCl_3$, 500 MHz): δ (ppm), 8.81 (s, 4H, $H_{3'}$ and $H_{5'}$), 8.70 (ddd, 4H, H_6 and $H_{6''}$, $J_{H6\text{-}H5}$ = 4.8 Hz, J_{H6-H4} = 1.7 Hz, J_{H6-H3} = 0.9 Hz), 8.68 (dt, 4H, H_3 and $H_{3''}$, J_{H3-H4} = 7.7 Hz, J_{H3-H5} = 1.2 Hz), 8.19 (t, 2H, H_d, $J_{Hd-Ha\ (Hc)}$ = 1.7 Hz), 7.94−7.92 (m, 3H, H_a or H_c and H_e), 7.91 (d, 2H, H_f, J_{Hf-He} = 1.6 Hz), 7.88 (td, 4H, H_4 et $H_{4''}$, $J_{H4-H3\ (H5)}$ = 7.7 Hz, J_{H4-H6} = 1.7 Hz), 7.82 (ddd, 2H, H_a or H_c, $J_{Ha\ (Hc)-Hb}$ = 7.7 Hz, $J_{Ha\ (Hc)-Hd}$ = 1.7 Hz, J_{Ha-Hc} = 1.1 Hz), 7.77 (dd, 2H, H_g, J_{Hg-Hh} = 7.7 Hz, J_{Hg-Hi} = 1.7 Hz), 7.64 (t, 2H, H_b, $J_{Hb-Ha\ (Hc)}$ = 7.7 Hz), 7.50 (t, 2H, H_h, $J_{Hh-Hg\ (Hi)}$ = 7.7 Hz), 7.40 (tt, 1H, H_i, J_{Hi-Hh} = 7.7 Hz, J_{Hi-Hg} = 1.7 Hz), 7.34 (ddd, 4H, H_5 and $H_{5''}$, J_{H5-H4} = 7.7 Hz, J_{H5-H6} = 4.8 Hz, J_{H5-H3} = 1.2 Hz). ^{13}C NMR ($CDCl_3$, 75 MHz): δ (ppm), 156.24, 156.02, 150.53, 149.18, 142.73, 142.36, 142.17, 141.13, 139.42, 137.12, 129.64, 129.01, 128.39, 127.67, 126.87, 126.55, 125.85, 125.79, 124.00, 121.57, 119.38. HRMS (APCI): m/z calculated for $[C_{54}H_{36}N_6 + H]^+$, 769.3071; found: 769.3074.

4,4′-Bis(4,4,5,5-tetramethyl-1,3,2-dioxaborolan-2-yl)-1,1′-biphenyl (1). To a mixture of 4,4′-dibromo-1,1′-biphenyl (0.5000 g, 1.602 mmol, 1 equiv), Bis(pinacolato)diboron (0.8546 g, 3.365 mmol, 2.1 equiv), KOAc (0.9438 g, 9.615 mmol, 6 equiv) and $[Pd(dppf)Cl_2].CH_2Cl_2$ (0.1308, 0.1602 mmol, 0.1 equiv) was added anhydrous DMSO (15 mL). The reaction mixture was degassed by three freeze−pump−thaw cycles and heated to 80 °C under argon atmosphere for 10h. 50 mL of toluene was added and the reaction mixture is extracted five times with 100 mL of water, the organic layer is dried over $MgSO_4$ and solvent removed to afford 1 (0.6051 g, 93%) as a gray powder. ^{1}H NMR ($CDCl_3$, 300 MHz): δ (ppm), 7.88 (d, 4H, H_a or H_b, J_{Ha-Hb} = 8.2 Hz), 7.63 (d, 4H, H_a or H_b, J_{Ha-Hb} = 8.2 Hz), 1.36 (s, 24H, H_c). ^{13}C NMR ($CDCl_3$, 75 MHz): δ (ppm), 135.38, 126.65, 83.98, 25.03. MS (EI): m/z calculated for $[C_{24}H_{32}B_2O_4]$+, 406.2; found: 406.0.

3,3‴,5,5‴-Tetrabromo-1,1′:4′,1″:4″,1‴-quaterphenyl (2). To **1** (1.3168 g, 3.266 mmol, 1 equiv), 1,3,5-Tribromobenzene (8.226 g, 26.13 mmol, 8 equiv) and $[Pd(PPh_3)_2Cl_2]$ (0.2293 g, 0.3266 mmol, 0.1 equiv) was added a mixture of toluene/aqueous K_2CO_3 2 M (45 mL, 2/1). The reaction mixture was degassed by three freeze−pump−thaw cycles and heated to 100 °C under argon atmosphere for 18h. 50 mL of water were added and the reaction mixture was extracted three times with 100 mL of toluene; organic layers were combined, dried over $MgSO_4$ and solvents removed under vacuum. The off-white powder was purified by column chromatography on SiO_2 ($CHCl_3$/cyclohexane: 4/1) and washed one time with acetone to afford **2** (0.7256 g, 36%) as a white powder. ^{1}H NMR ($CDCl_3$, 500 MHz): δ (ppm), 7.74−7.70 (m, 8H, H_a and H_b), 7.66 (t, 2H, H_d, J_{Hd-Hc} = 1.7 Hz), 7.65−7.62 (m, 4H, H_c). ^{13}C NMR ($CDCl_3$, 75 MHz): δ (ppm), 144.30, 140.50, 137.72, 132.89, 129.01, 127.80, 127.75, 123.52. MS (EI): m/z calculated for $[C_{24}H_{14}Br_4]^+$, 621.8; found: 621.6.

(L5): To **2** (0.1500 g, 0.2412 mmol, 1 equiv), (3-([2,2′:6′,2″-terpyridin]-4′-yl)phenyl)boronic acid (0.6299 g, 1.446 mmol, 6 equiv) and Na_2CO_3 (0.3067 g, 2.894 mmol, 12 equiv) was added a mixture of water/tert-butanol/toluene (80 mL, 3/2/15). The reaction mixture was degassed by four freeze−pump−thaw cycles; after the third cycle, when the reaction mixture being frozen, the $[Pd(PPh_3)_2Cl_2]$ (0.0406 g, 0.0579 mmol, 0.24 equiv) was added, and one more freeze−pump−thaw cycle was done. The reaction mixture was heated to 110 °C under argon atmosphere during 3 days. 100 mL of water were added to the reaction mixture and the aqueous phase was extracted five times with 150 mL CH_2Cl_2. Organic layers were combined, dried over $MgSO_4$ and solvents removed. The off-white powder was dissolved in 10 mL of hot toluene and 100 mL of MeOH were added to induce the precipitation of the desired product. The solid was washed two times with MeOH and one time with a MeOH/CH_2Cl_2 (9/1) mixture to afford **L5** (0.0714g, 19%) as a white powder. ^{1}H NMR ($CDCl_3$/$(CF_3)_2$CHOH:20/1, 500 MHz): δ (ppm), 8.64 (ddd, 8H, H_6 and $H_{6''}$, J_{H6-H5} = 5.0 Hz, J_{H6-H4} = 1.6 Hz, J_{H6-H3} = 0.8 Hz), 8.49 (s, 8H, $H_{3'}$ and $H_{5'}$), 8.44 (d, 8H, H_3 and $H_{3''}$, J_{H3-H4} = 7.9 Hz), 8.19 (s, 4H, H_f), 8.00−7.96 (m, 14H, H_e, H_d, H_4 and $H_{4''}$), 7.93 (d, 4H, H_a or H_c, $J_{Ha\ (Hc)-Hb}$ = 7.7 Hz), 7.90−7.87 (m, 8H, H_a or H_c and H_g or H_h), 7.81 (d, 4H, H_g or H_h, J_{Hg-Hh} = 8.4 Hz), 7.68 (t, 4H, H_b, $J_{Hb-Ha\ (Hc)}$ = 7.7 Hz), 7.47 (ddd, 8H, H_5 and $H_{5''}$, J_{H5-H4} = 7.5 Hz, J_{H5-H6} = 5.0 Hz, J_{H5-H3} = 1.1 Hz). ^{13}C NMR ($CDCl_3$/$(CF_3)_2$CHOH:20/1, 75 MHz): δ (ppm), 156.20, 156.00, 151.45, 148.72, 142.33, 138.53, 129.95, 128.84, 128.06, 127.74, 126.81, 126.43, 125.73, 124.64, 120.61. HRMS (APCI): m/z calculated for $[C_{108}H_{70}N_{12} + H]^+$, 1535,5899 ; found: 1535.8919.

[Ru$_3$(L1)(tpy)$_3$](PF$_6$)$_6$ (C1). To **L1** (0.0145 g, 0.0188 mmol, 1 equiv) and [Ru(tpy)Cl_3] (0.0324 g, 0.0324 mmol, 3.9 equiv) was added a mixture of isopropanol/water (20 mL, 1:1) and N-ethylmorpholine (0.5 mL). The reaction medium was heated to 90 °C for 3 days and cooled down to room temperature. An excess of aqueous ammonium hexafluorophosphate was added to the solution and the resulting precipitate was collected and washed with water. The solid was purified by flash chromatography on SiO_2 (acetonitrile/saturated aqueous KNO_3/water:7/1/0.5), precipitated by addition of an excess of aqueous ammonium hexafluorophosphate and washed three times with water to afford **C1** (0.0170 g, 34%) as a dark red solid. ^{1}H NMR (CD_3CN, 500 MHz): δ (ppm),9.72 (s, 2H, H_c or H_d), 9.69 (s, 2H, H_c or H_d), 9.23 (s, 4H, $H_{3'}$ and $H_{5'}$), 8.93 (d, 2H, $H_{B3'}$ and $H_{B5'}$, $J_{HB3'\ (HB5')\text{-}HB4''}$ = 8.0 Hz), 8.78 (d, 8H, H_3, H $_{3''}$, $H_{A3'}$ and $H_{A5'}$, $J_{H3\text{-}H4}$ = 7.9 Hz, $J_{HA3'\ (HA5')\text{-}HA4'}$ = 7.9 Hz), 8.66 (d, 2H, H_A, $J_{Ha\text{-}Hb}$ = 7.7 Hz), 8.58 (t, 1H, $H_{B4'}$, $J_{HB4'\text{-}HB3'\ (HB5')}$ = 8.0 Hz), 8.51 (m, 6H, H_e, H_{A3} and $H_{A3''}$), 8.44 (t, 2H, $H_{A4'}$, $J_{HA4'\text{-}HA3'\ (HA5')}$ = 7.9 Hz), 8.04 (m 4H, H_b, H_{B4} and $H_{B4''}$), 7.96 (t, 4H, H_4 and $H_{4''}$, $J_{H4\text{-}H3\ (H5)}$ = 7.9 Hz), 7.91 (t, 4H, H_{A4} and $H_{A4''}$, $J_{HA4\text{-}HA3\ (HA5)}$ = 7.9 Hz), 7.80 (t, 2H, H_f, $J_{Hf\text{-}He\ (Hg)}$ = 7.3 Hz), 7.77 (d, 2H, H_{B3} and $H_{B3''}$, $J_{HB3\text{-}HB4}$ = 5.5 Hz), 7.71 (m, 3H, H_g, H_{B6} and $H_{B6''}$), 7.37 (d, 8H, H_6, $H_{6''}$, H_{A6} and $H_{A6''}$, J_{H6-H5} = 4.7 Hz, $J_{HA6\text{-}HA5}$ = 4.7 Hz), 7.33 (m, 2H, H_{B5} and $H_{B5''}$), 7.21 (m, 4H, H_5 and $H_{5''}$), 7.14 (m, 4H, H_{A5} and $H_{A5''}$). MS (ESI): m/z calculated for $[C_{96}H_{66}N_{18}Ru_3P_2F_{12}]^{4+}$, 443.82; found: 443.80, m/z calculated for $[C_{96}H_{66}N_{18}Ru_3P_1F_6]^{5+}$, 355.06; found: 355.05, m/z calculated for $[C_{96}H_{66}N_{18}Ru_3]^{6+}$, 295.88; found: 295.87. MS (MALDI): m/z calculated for $[C_{96}H_{66}N_{18}Ru_3P_5F_{30}]^+$, 2500.11; found: 2499.99, m/z calculated for $[C_{96}H_{66}N_{18}Ru_3P_4F_{24}]^+$, 2355.02; found: 2355.15, m/z calculated for $[C_{96}H_{66}N_{18}Ru_3P_3F_{18}]^+$, 2210.08; found: 2210.18, m/z calculated for $[C_{96}H_{66}N_{18}Ru_3P_2F_{12}]^+$, 2065.10; found: 2065.22.

[Ru$_4$(L2)(tpy)$_4$](PF$_6$)$_8$ (C2). To **L2** (0.0200 g, 0.0185 mmol, 1 equiv) and [Ru(tpy)Cl_3] (0.0436 g, 0.0986 mmol, 5.33 equiv) was added a mixture of isopropanol/water (20 mL, 1:1) and N-ethylmorpholine (1 mL). The reaction medium was heated to 90 °C for 3 days and cooled down to room temperature. An excess of aqueous ammonium hexafluorophosphate was added to the solution and the resulting precipitate was collected and washed with water. The solid was purified by flash chromatography on SiO_2 (Acetonitrile/saturated aqueous KNO_3/water:7/1/0.75), precipitated by addition of an excess of aqueous ammonium hexafluorophosphate and washed three times

DOI: 10.1021/acs.inorgchem.7b03040
Inorg. Chem. XXXX, XXX, XXX−XXX

with water to afford **C2** (0.0146 g, 22%) as a dark red solid. ^{1}H NMR (CD_3CN, 500 MHz): δ (ppm), 9.77 (s, 2H, H_c or H_d), 9.68 (s, 2H, H_c or H_d), 9.22 (s, 4H, $H_{3'}$ and $H_{5'}$), 9.13(s, 2H, $H_{e'}$), 8.97 (d, 2H, $H_{B3'}$ and $H_{B5'}$, $J_{HB3'\ (HB5')\text{-}HB4''}$ = 8.3 Hz), 8.83−8.69 (m, 16H, H_a, H_e, $H_{d'}$, H_3, $H_{3''}$, $H_{A3'}$, $H_{A5'}$, $H_{C3'}$ and $H_{C5'}$), 8.62 (t, 1H, $H_{B4'}$, $J_{HB4'-HB3'\ (HB5')}$ = 8.3 Hz), 8.54 (d, 6H, H_{A3}, $H_{A3''}$, H_{C3} and $H_{C3''}$, $J_{HA3\text{-}HA4}$ = 8.0 Hz, $J_{HC3\text{-}HC4}$ = 8.0 Hz), 8.41−8.41 (m, 5H, $H_{f'}$, $H_{A4'}$ and $H_{C4'}$), 8.33 (d, 2H, H_f, J_{Hf-He} = 8.2 Hz), 8.29 (d, 2H, $H_{g'}$, $J_{g'\text{-}He'}$ = 8.3 Hz), 8.10 (t, 2H, $H_{c'}$, $J_{Hc'\text{-}Hb'(Hd')}$ = 7.5 Hz), 8.06−7.93 (m, 14H, H_b, H_4, $H_{4''}$, H_{A4}, $H_{A4''}$, H_{B4}, $H_{B4''}$, H_{C4} and $H_{C4''}$), 7.83 (d, 2H, H_{B3} and $H_{B3''}$, $J_{HB3\text{-}HB4}$= 5.9 Hz), 7.78 (d, 2H, $H_{a'}$, $J_{Ha'\text{-}Hb'}$= 5.4 Hz), 7.47 (d, 2H, H_{C6} and $H_{C6''}$, $J_{HC6\text{-}HC5}$= 5.3 Hz), 7.45−7.36 (m,12H, $H_{b'}$, H_6, $H_{6''}$, H_{A6}, $H_{A6''}$, H_{B6} and $H_{B6''}$), 7.28−7.16 (m, 12H, H_5, $H_{5''}$, H_{A5}, $H_{A5''}$, H_{B5}, $H_{B5''}$, H_{C5} and $H_{C5''}$). MS (ESI): m/z calculated for $[C_{132}H_{90}N_{24}Ru_4P_2F_{12}]^{6+}$, 402.57; found: 402.73, m/z calculated for $[C_{132}H_{90}N_{24}Ru_4PF_6]^{7+}$, 345.20; found: 345.06, m/z calculated for $[C_{132}H_{90}N_{24}Ru_4]^{8+}$, 302.05; found: 302.18, m/z calculated for $[C_{132}H_{90}N_{24}Ru_4]^{9+}$, 268.71; found: 268.48. MS (MALDI): m/z calculated for $[C_{132}H_{90}N_{18}Ru_4P_7F_{42}]^+$, 3432.15; found: 3432.22.

*$[Ru_6(L3)(tpy)_6](PF_6)_{12}$ (**C3**).* To **L3** (0.0130g, 0.0084 mmol, 1 equiv) and $[Ru(tpy)Cl_3]$ (0.0297 g, 0.0674 mmol, 8 equiv) was added a mixture of isopropanol/water (20 mL, 1:1) and N-ethylmorpholine (1 mL). The reaction medium was heated to 90 °C for 3 days and cooled down to room temperature. An excess of aqueous ammonium hexafluorophosphate was added to the solution and the resulting precipitated was collected and washed with water. The solid was purified by flash chromatography on SiO_2 (Acetonitrile/saturated aqueous KNO_3/water:7/2/2), precipitated by addition of an excess of aqueous ammonium hexafluorophosphate and washed three times with water to afford **C3** (0.0049 g, 11%) as a dark red solid. ^{1}H NMR (CD_3CN, 500 MHz): δ (ppm), 9.91 (s, 4H, H_c or H_d), 9.75 (s, 4H, H_c or H_d), 9.30 (s, 8H, $H_{3'}$ and $H_{5'}$), 8.94 (d, 4H, $H_{B3'}$ and $H_{B5'}$, $J_{HB3'\ (HB5')\text{-}HB4'}$= 8.2 Hz), 8.82 (d, 8H, H_3 and $H_{3''}$, J_{H3-H4}= 8.0 Hz), 8.80−8.75 (m, 12H, H_e, $H_{A3'}$ and $H_{A5'}$), 8.67 (d, 4H, H_a, $J_{Ha\text{-}Hb}$= 8.2 Hz), 8.57 (t, 2H, $H_{B4'}$ and $H_{B5'}$, $J_{HB4'\text{-}HB3'\ (HB5')}$= 8.2 Hz), 8.50 (d, 8H, H_{A3} and $H_{A3''}$, $J_{HA3\text{-}HA4}$= 8.0 Hz), 8.43 (t, 4H, $H_{A4'}$, $J_{HA4'\text{-}HA3'\ (HA5')}$= 8.2 Hz), 8.26 (d, 4H, H_f, J_{Hf-He}= 8.2 Hz), 8.06−8.02 (m, 8H, H_b, H_{B4} and $H_{B4''}$), 7.95 (t, 8H, H_4 and $H_{4''}$, $J_{H4-H3\ (H5)}$= 8.0 Hz), 7.89 (t, 8H, H_{A4} and $_{HA4''}$, $J_{HA4\text{-}HA3\ (HA5)}$= 8.0 Hz), 7.77 (d, 4H, H_{B3} and $H_{B3''}$, $J_{HB3\text{-}HB4}$= 5.8 Hz), 7.74 (d, 4H, H_{B6} and $H_{B6''}$, $J_{HB6\text{-}HB5}$= 5.4 Hz), 7.39 (d, 8H, H_{A6} and $H_{A6''}$, $J_{HA6\text{-}HA5}$= 5.4 Hz), 7.36 (d, 8H, H_6 and $H_{6''}$, J_{H6-H5}= 5.4 Hz), 7.33−7.31 (m, 4H, H_{B5} and $H_{B5''}$), 7.18−7.15 (m, 8H, H_5 and $H_{5''}$), 7.14−7.11 (m, 8H, H_{A5} and $H_{A5''}$). MS (ESI): m/z calculated for $[C_{192}H_{130}N_{36}Ru_6]^{12+}$, 295.71; found: 295.70.

*$[Ru_2(L4)(tpy)_2](PF_6)_4$ (**C4**).* To **L4** (0.0160g, 0.0208 mmol, 1 equiv) and $[Ru(tpy)Cl_3]$ (0.0244 g, 0.0554 mmol, 2.66 equiv) was added a mixture of water/isopropanol/hexafluoroisopropanol (16 mL, 4:3:1) and N-ethylmorpholine (0.5 mL). The reaction media was heated to 90 °C for 3 days and cooled down to room temperature. An excess of aqueous ammonium hexafluorophosphate was added to the solution and the resulting precipitate was collected and washed with water. The solid was purified by a first flash chromatography on SiO_2 (Acetonitrile/saturated aqueous KNO_3/water:7/1/0.5), precipitated by addition of an excess of aqueous ammonium hexafluorophosphate and purified again by a second flash chromatography on SiO_2 (Acetonitrile/saturated aqueous KNO_3/water:7/2/2), precipitated by addition of an excess of aqueous ammonium hexafluorophosphate and washed three times with water to afford **C4** (0.0263 g, 88%) as a red solid. ^{1}H NMR (CD_3CN, 500 MHz): δ (ppm), 9.18 (s, 4H, $H_{3'}$ and $H_{5'}$), 8.79−8.75 (m, 6H, H_d, $H_{A3'}$ and $H_{A5'}$), 8.71 (d, 4H, H_3 and $H_{3''}$, $J_{H3\ H4}$= 8.0 Hz), 8.51 (d, 4H, H_{A3} and $H_{A3''}$, $J_{HA3\ HA4}$= 8.0 Hz), 8.47 (t, 1H, H_e, $J_{He\ Hf}$= 1.6 Hz), 8.42 (t, 2H, $H_{A4'}$, $J_{HA4'\ HA3'(HA5')}$= 8.2 Hz), 8.30−8.26 (m, 4H, H_a or H_c and H_f), 8.22 (d, 2H, H_a or H_c, $J_{Ha\ (Hc)\text{-}Hb}$= 7.8 Hz), 8.00 (dd, 2H, H_g, $J_{Hg\text{-}Hh}$= 7.8 Hz, $J_{Hg\ Hi}$= 1.1 Hz), 7.93 (t, 2H, H_b, $J_{Hb\text{-}Ha\ (Hc)}$= 7.8 Hz), 7.89−7.84 (m, 8H, H_4, $H_{4''}$, H_{A4} and $H_{A4''}$), 7.60 (t, 2H, H_h, $J_{Hh\text{-}Hg\ (Hi)}$= 7.8 Hz), 7.50 (tt, 1H, H_i, $J_{Hi\text{-}Hh}$= 7.8 Hz, $J_{Hi\text{-}Hg}$= 1.1 Hz), 7.45 (dd, 4H, H_6 and $H_{6''}$, J_{H6-H5}= 5.6 Hz, J_{H6-H4}= 0.7 Hz), 7.35 (dd, 4H, H_{A6} and $H_{A6''}$, $J_{HA6\text{-}HA5}$= 5.6 Hz, J_{H6-H4}= 0.7 Hz), 7.13 (m, 4H, H_{A5} and $H_{A5''}$), 7.07 (m, 4H, H_5 and $H_{5''}$). MS (MALDI): m/z calculated for $[C_{84}H_{58}N_{12}Ru_2P_3F_{18}]^+$, 1873.20; found: 1873.12, $[C_{84}H_{58}N_{12}Ru_2P_2F_{12}]^+$, 1727.23; found: 1727.19. MS (ESI): m/z calculated for $[C_{84}H_{58}N_{12}Ru_2PF_6]^{3+}$, 479.10; found: 479.09, m/z calculated for $[C_{84}H_{58}N_{12}Ru_2]^{4+}$, 359.58; found: 360.07, m/z calculated for $[C_{84}H_{58}N_{12}Ru_2]^{5+}$, 287.86; found: 287.66.

*$[Ru_4(L5)(tpy)_4](PF_6)_8$ (**C5**).* To **L5** (0.0150g, 0.00977 mmol, 1 equiv) and $[Ru(tpy)Cl_3]$ (0.0243 g, 0.0553 mmol, 5.66 equiv0.) was added a mixture of water/isopropanol/hexafluoroisopropanol (16 mL, 4:3:1) and N-ethylmorpholine (1 mL). The reaction medium was heated to 90 °C for 3 days and cooled down to room temperature. An excess of aqueous ammonium hexafluorophosphate was added to the solution and the resulting precipitated was collected and washed with water. The solid was purified by a flash chromatography on SiO_2 (Acetonitrile/saturated aqueous KNO_3/water:7/1/0.5), precipitated by addition of an excess of aqueous ammonium hexafluorophosphate and washed three time, with water to afford **C5** (0.0171 g, 43%) as a red solid. ^{1}H NMR (CD_3CN, 500 MHz): δ (ppm), 9.20 (s, 8H, $H_{3'}$ and $H_{5'}$), 8.82 (s, 4H, H_d), 8.77 (d, 8H, $H_{A3'}$ and $H_{A5'}$, $J_{H3'\text{-}H4'}$ = 8.1 Hz), 8.72 (d, 8H, H_3 and $H_{3''}$, J_{H3-H4} = 8.1 Hz), 8.53 (s, 2H, H_e), 8.49 (d, 8H, H_{A3} and $H_{A3''}$, $J_{HA3\text{-}HA4}$ = 8.1 Hz), 8.43 (t, 4H, $H_{A4'}$, $J_{HA4'\text{-}HA3'\ (HA5')}$ = 8.2 Hz), 8.34 (d, 4H, H_f, J_{Hf-He} = 1.0 Hz), 8.29 (d, 4H, H_a or H_c, $J_{Ha\ (Hc)\text{-}Hb}$ = 7.7 Hz), 8.25 (d, 4H, H_a or H_c, $J_{Ha\ (Hc)\text{-}Hb}$ = 8.2 Hz 8.16 (d, 4H, H_g or H_h, $J_{Hg\text{-}Hh}$ = 8.2 Hz), 8.02 (d, 4H, H_g or H_h, $J_{Hg\text{-}Hh}$ = 8.2 Hz), 7.95 (d, 4H, H_b, $J_{Hb\text{-}Ha\ (Hc)}$ = 7.7 Hz), 7.85 (t, 16H, H_4, $H_{4''}$, H_{A4} and $H_{A4''}$, $J_{H4-H3\ (H5)}$ = 8.1 Hz), 7.45 (d, 8H, H_6 and $H_{6''}$, J_{H6-H5} = 5.4 Hz), 7.35 (d, 8H, H_{A6} and $H_{A6''}$, $J_{HA6\text{-}HA5}$ = 5.4 Hz), 7.14−7.09 (m, 8H, H_{A4} and $H_{A4''}$), 7.08−7.03 (m, 8H, H_4 and $H_{4''}$). MS (MALDI): m/z calculated for $[C_{168}H_{114}N_{24}Ru_4P_7F_{42}]^+$, 3888.34; found: 3888.43. MS (ESI): m/z calculated for $[C_{168}H_{114}N_{24}Ru_4P_2F_{12}]^{6+}$, 526.91; found: 527.09, m/z calculated for $[C_{168}H_{114}N_{24}Ru_4PF_6]^{7+}$, 431.08; found: 431.22, m/z calculated for $[C_{168}H_{114}N_{24}Ru_4]^{8+}$, 359.20; found: 359.20.

RESULTS AND DISCUSSION

Synthesis of the Multiterpyridine Analogs. As stated in the Introduction, the synthesis of the multiterpyridines **L1**, **L2**, and **L3** has been developed recently in our laboratory. We first focused on the synthesis of ligands **L4** and **L5**, analogs of ligands **L1** and **L3**, respectively, where the *central terpyridine* binding site is absent. The analogs of the ligand **L1**, *i.e.* **L4** (Scheme 2a), were obtained by a Suzuki cross-coupling reaction between the 3,5-dibromobiphenyl[46] and the (3-([2,2′:6′,2″-terpyridin]-4′-yl)phenyl)boronic acid.[47] Concerning the ligand **L5**, a different synthetic route was developed (Scheme 2b). First a Miyaura cross-coupling reaction[61] between 4,4′-dibromobiphenyl and bis(pinacolato)diboron in anhydrous conditions gave the pinacolate ester **1**, which was then reacted with an excess of 1,3,5-tribromobenzene via a Suzuki-reaction in order to give predominantly the intermediate **2.** A quadruple Suzuki-reaction using the intermediate **2** and the (3-([2,2′:6′,2″-terpyridin]-4′-yl)phenyl)boronic acid gave the desired tetradentate ligand **L5**. All multiterpyridine analogs and new intermediates have been characterized by ^{1}H and ^{13}C NMR spectroscopy and high resolution mass spectrometry (Figure S1−S12).

Synthesis of the Multiterpyridine Ru(II) Complexes. With the five ligands **L1−5** in hand, we focused on the synthesis of multinuclear Ru(II) complexes (Scheme 1). The paramagnetic precursor $[Ru(tpy)Cl_3]$ was synthesized by refluxing 2,2′:6′,2″-terpyridine with $RuCl_3$ in ethanol according to the literature.[62] The complexes **C1−C3** were synthesized by refluxing the appropriate ligand with $[Ru(tpy)Cl_3]$ in the presence of *N*-ethylmorpholine as reducing agent in a water/isopropanol mixture, yielding a deep red mixture.[36] Concerning complexes **C4** and **C5**, the extremely low solubility of the ligands **L4** an **L5** in isopropanol does not allow the formation of the complexes according to previous conditions. The use of

DOI: 10.1021/acs.inorgchem.7b03040
Inorg. Chem. XXXX, XXX, XXX−XXX

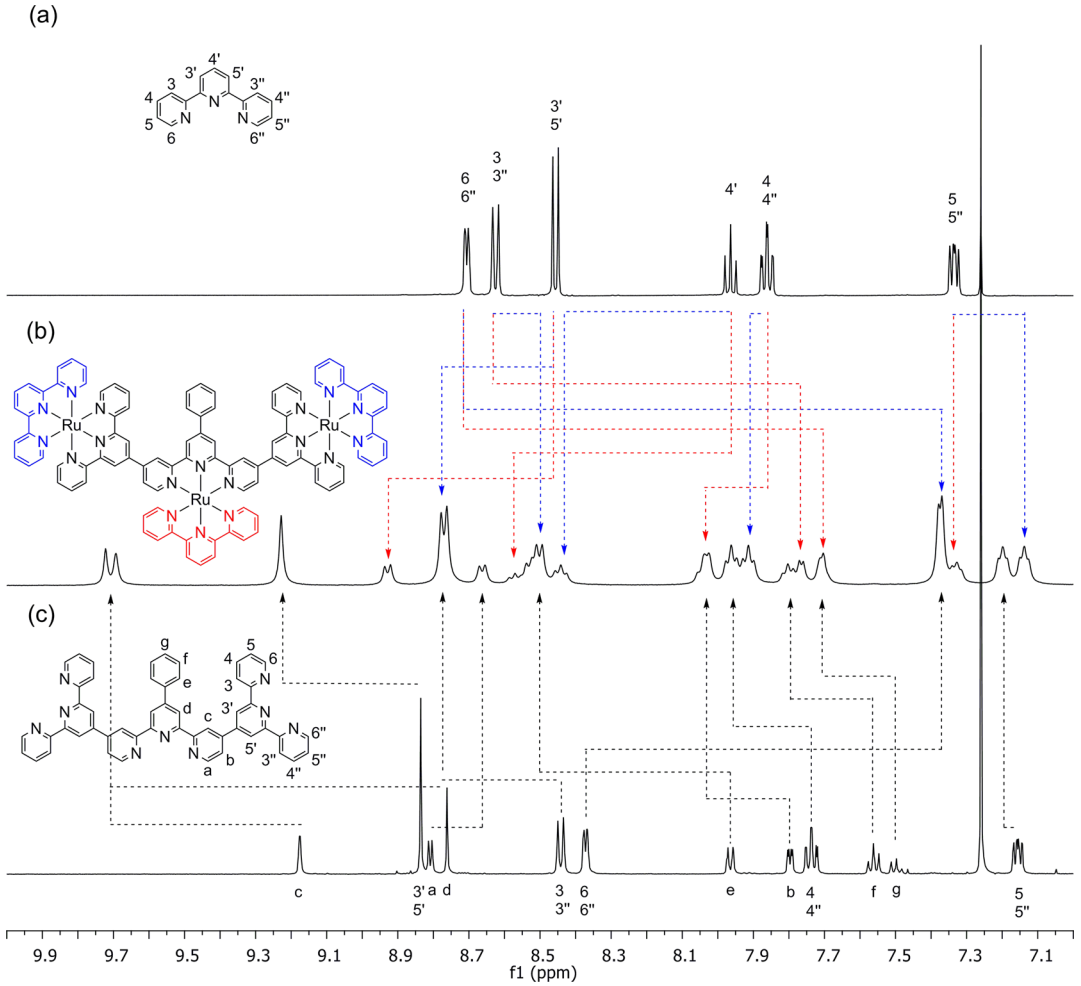

Figure 1. ^{1}H NMR (500 MHz, 298 K) spectra of (a) the ligand 2,2′:6′,2″-terpyridine in $CDCl_3$, (b) complex **C1** in CD_3CN, and (c) ligand **L1** in $CDCl_3$.

hexafluoroisopropanol (HFIP) as an additive for the solvent mixture allows the solubilization of the ligands and thus the synthesis of the complexes. At the end of the reaction, addition of saturated aqueous ammonium hexafluorophosphate led to the precipitation of a red solid, which was purified by flash chromatography on silica with an acetonitrile/saturated aqueous KNO_3/water mixture as eluent. Due to their large positive charge, the complexes tend to be partially absorbed on the silica, which led to complexes loss during the purification and low yields. The yield of complexation and purification varies from good to low (88−11%), with the complexes without the central chelating site (**C4** and **C5**) having better yield than the others (**C1**−**C3**), in agreement with previous reports[42,63] which showed that the more closely positioned the binding sites are, the lower the yield. Furthermore, the yield of the synthesis also decreases as the number of Ru(II) centers increases.

^{1}H NMR Characterization of the Complexes. Thanks to the use of terpyridine ligand as chelation moiety, no stereoisomers are generated during the reaction, easing the characterization of all the complexes by ^{1}H NMR spectroscopy. All peaks in the ^{1}H NMR spectra were fully assigned. The assignment of the different peaks was realized by performing ^{1}H−^{1}H COSY spectra and comparison to the free ligand (Figure 1). The signals of all tepyridine units are impacted by the complexation of the Ru(II). The most noticeable effect of the complexation of the Ru(II) center to a terpyridine core is the necessity for the tpy ligand to switch from a *trans* to a *cis* conformation;[36] in *trans* conformation, the lone pair of the nitrogen atom deshields the 3′ and 5′ protons, whereas that is not the case in the *cis* conformation. For the complex **C1**, the protons 3′ and 5′ of the two chemically nonequivalent terpyridines (blue and red Figure 1) are downfield of 0.31 and 0.15 ppm, respectively; for the two different terpyridine units of the ligand **L1** this downfield is 0.94 (H_d) and 0.39 ($H_{3',5'}$) ppm. The other noticeable effect of the complexation is the upfield of the protons 6 and 6″; for the ancillary terpyridine this upfield is −1.37 and −1.01 ppm, and for the ligand **L1** this upfield is −1 ppm. It is interesting to note that the proton H_a of the ligand **L1** shows only an upfield of −0.15 ppm which is surprisingly small. The same observation may be done for the complexes **C2**, **C3**, **C4**, and **C5**. The comparison between the ^{1}H NMR spectra of the complexes **C1** and **C3** shows only small changes (Figure 2); only the protons H_e and H_f are upfield when we switch from the complex **C1** to **C3**, and the proton H_g disappears. The same observations are made for complexes **C4** and **C5**.

Mass Characterization of the Complexes. All the complexes were also characterized by mass spectrometry using both available ionization sources, i.e. matrix assisted laser desorption/ionization (MALDI) and electrospray ionization (ESI). First, the MALDI-ToF technique allows for all our

DOI: 10.1021/acs.inorgchem.7b03040
Inorg. Chem. XXXX, XXX, XXX−XXX

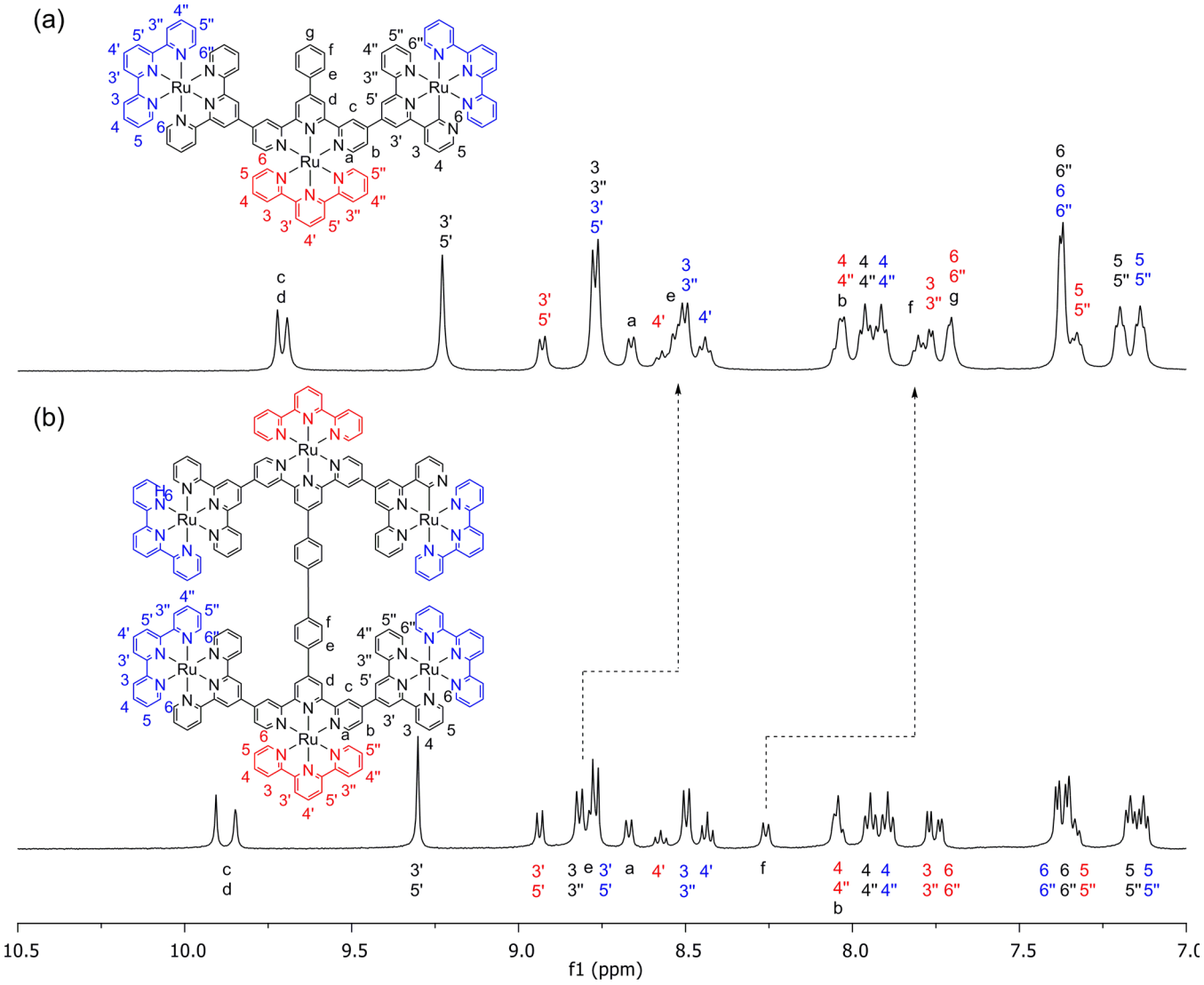

Figure 2. ^{1}H NMR (500 MHz, 298 K) spectra in CD_3CN of (a) **C1** and (b) **C3**.

complexes (except the complex **C3**) the observation of the singly charged ions, corresponding to the entire complex having lost only one PF_6^- counterion. Nevertheless, it is worth noticing that other singly charged ions having lost multiple PF_6^- are also observed in the mass spectra. Indeed, during the MALDI process, free electrons can be produced in the plume and capped by multiple charged ions,[64] inducing some reduction reactions, and, as a consequence, detect those complexes singly charged but presenting different number of hexafluorophosphate counterions (Figure S23–S31). On the other hand, ESI allows, for all the complexes, the detection of multicharged complexes with a variable number of hexafluorophosphate counterion losses (Figures S24, S26–S27, S29, and S31). All the different complexes have been characterized by using both techniques, confirming the success of the syntheses.

Electrochemical Measurements. The results of the cyclic voltammetry are reported in Table 1. The complexes **C1**–**C5** show a single reversible oxidation wave corresponding to the Ru(II)/Ru(III) oxidation process(es) for all the Ru(II) centers, which thus all occur at the same potential, similar to the one of the reference complex $[Ru(tpy)_2]^{2+}$. The presence of one single oxidative process for multinuclear complexes is indicative of weak intermetal interactions between the different Ru(II) centers. In reduction, a different behavior can clearly be observed for the different complexes. Indeed, although complexes **C4** and **C5** exhibit two reduction waves at similar potentials as for the complex $[Ru(tpy)_2]^{2+}$, the situation is different for complexes **C1**–**C3**. In these cases, a new reduction wave at a less negative potential is detected; this reduction wave is attributed to the reduction of the bridging terpyridine unit.

Table 1. Oxidation and Reduction Potential[a]

Complex	E_{Ox}[b]	E_{Red}[c]		
C1	+1.39	−0.64	−0.96	−1.30
C2	+1.39	−0.69	−0.94	−1.33
C3	+1.39	−0.69	n.d.	n.d.
C4	+1.35		−1.01	−1.27
C5	+1.43[c]		−1.01	−1.26
$[Ru(tpy)_2]^{2+}$	+1.37		−1.03	−1.27

[a] $E_{1/2}$(V) vs Ag/AgCl. [b] In acetonitrile. [c] In DMF.

The electrochemical measurements reveal thus two different behaviors. (i) Complexes **C4** and **C5** have electrochemical properties similar to that of the reference complex $[Ru(tpy)_2]^{2+}$ and could thus be considered as *simple* polynuclear assemblies of the reference unit $[Ru(tpy)_2]^{2+}$. (ii) On the contrary, for

DOI: 10.1021/acs.inorgchem.7b03040
Inorg. Chem. XXXX, XXX, XXX–XXX

complexes **C1**−**C3** the multiterpyridine bridging ligand induces the appearance of a new reduction wave at higher potential; the resulting complexes possess thus clearly distinct properties compared to the reference complex. Thanks to these observations, we could expect that complexes **C1**−**C3** will present different photophysical properties.

UV/Visible Spectroscopy. The absorption spectra of complexes **C1**−**C5** and the reference $[Ru(tpy)_2](PF_6)_2$ are shown in Figure 3, and the maxima of absorption and the molar extinction coefficient are gathered in Table 2. The intense and sharp bands localized in the UV part of the spectra are attributed to ligand-centered (LC) $\pi-\pi^*$ transitions on the terpyridine ligands and the multitepyridine bridging ligands. The broad bands in the 400−650 nm visible region correspond to a metal-to-ligand charge-transfer (MLCT) transition between the Ru(II) ions and the ancillary ligands. Complexes **C4** and **C5** and the reference complex $[Ru(tpy)_2]^{2+}$ depict a very similar shape for this band, with the maxima of the MLCT band being only a little bit red-shifted for complexes **C4**−**C5** in comparison to $[Ru(tpy)_2]^{2+}$ and the molar extinction coefficient increases with the number of Ru(II) centers (Figure 3). In contrast, the MLCT transition for complexes **C1**−**C3** is not only slightly red-shifted in comparison to the reference $[Ru(tpy)_2]^{2+}$, but a bathochromic shoulder can be observed for the MLCT band. As for previous complexes, the molar extinction coefficient increases with the number of Ru(II) centers.

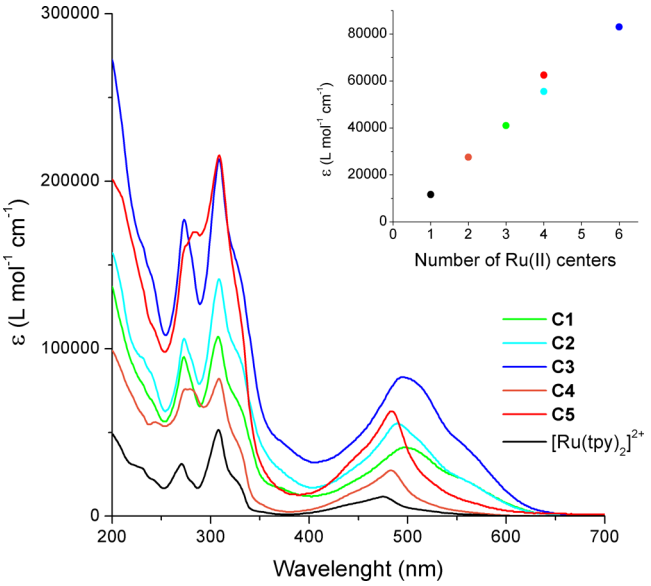

Figure 3. Absorption spectra in acetonitrile solution at 298 K. Inset: molar extinction coefficient of the maximum of the UV−visible MLCT band as a function of the number of Ru(II) centers of the different complexes.

The *central* terpyridine coordinating site in the ligands **L1**, **L2**, and **L3** seems thus to have considerable effects on the MLCT transition of the resulting complexes. The bathochromic absorbance of the MLCT of **C1**−**C3** suggests that a less energetic transition involving the *central* terpyridine coordinating site is present; for these complexes it can thus be stated that a more bathochromic transition corresponding to the MLCT transition between the different Ru(II) centers and the multiterpyridine bridging ligand is at stake. The similarity between the absorption spectra in the visible part of complexes **C4**−**C5** and the $[Ru(tpy)_2](PF_6)_2$ is in agreement with the crucial role played by the *central* terpyridine unit for complexes **C1**−**C3**. For all the complexes, the quasi linear relationship between the number of Ru(II) centers and the absorption coefficient for the MLCT absorption bands demonstrates that each chromophore is responsible for the absorption cross section; for polynuclear systems, this is consistent with the small electronic interaction between the different metallic centers.[65,66]

Emission Spectroscopy. The luminescence of the complexes in nitrile solvents was studied at 77 K in frozen media (Figure 4) and at 298 K (Figure 5). We checked that the emission properties of complexes **C1**−**C5** are independent with the wavelength of excitation and we demonstrated that the emission is solely due to our complexes and not an impurity by recording excitation spectra, which matched the absorption spectra of our complexes (see S38−S40).

At 77 K, all the complexes are luminescent. Complexes **C4** and **C5** have a maximum of emission at 624 nm, slightly red-shifted compared to the emission of reference $[Ru(tpy)_2]^{2+}$, the maximum of luminescence of which is located at 600 nm (Table 2). The increase of the number of Ru(II) centers from **C4** to **C5** has no influence over the maxima of emission. In contrast, for complexes **C1**−**C3**, the emission at 77 K is more bathochromic and the red-shift compared to $[Ru(tpy)_2]^{2+}$ increases with the number of Ru(II) centers. The presence of only one emission band for complexes **C1**, **C2**, and **C3** is very interesting. Indeed, complexes **C1** and **C3** possess two types of Ru(II) centers whereas complex **C2** presents three types of Ru(II) centers. If there were no interaction between Ru(II) centers, the emission spectra would present at least two (or

Table 2. Luminescence Properties of Complexes C1−C5 and Reference $[Ru(tpy)_2](PF_6)_2$ in Nitrile Solvents

	Absorption		Luminescence						
	298 K[a,b]			298 K[a]				77 K[c]	
Compound	λ_{max} (nm)	ε_{max} (M^{-1} cm^{-1})	λ_{ex} (nm)	λ_{max} (nm)	τ (ns)[c]	Φ_{em}[a,d]	10^{-4} k_r[a]	λ_{max} (nm)	τ (μs)
C1	497	41000	500	682	101.1 [119.2]	0.0014	1.4	670	12.0
C2	489	55500	500	684	81.9 [88.1]	0.0012	1.5	672	9.4
C3	495	83000	500	685	94.1 [101.2]	0.0016	1.7	678	8.2
C4	483	27500	480	639				624	10.6
C5	484	62500	480	639				624	4.8
$[Ru(tpy)_2]^{2+}$	475	11600	476	625		$\leq 5 \times 10^{-6}$[f]		600	10.9

[a]Air-equilibrated acetonitrile solution. [b]Only the absorption band in the visible region is indicated. [c]In brackets values for dearated acetonitrile solution. [d]$[Ru(bpy)_3]Cl_2$ in air-equilibrated acetonitrile used as reference (ϕ_{em} = 0.018) and excitation at 450 nm; uncertainty over the measures is estimated to be 20%. [e]Butyronitrile rigid matrix. [f]Data taken from ref 28.

DOI: 10.1021/acs.inorgchem.7b03040
Inorg. Chem. XXXX, XXX, XXX−XXX

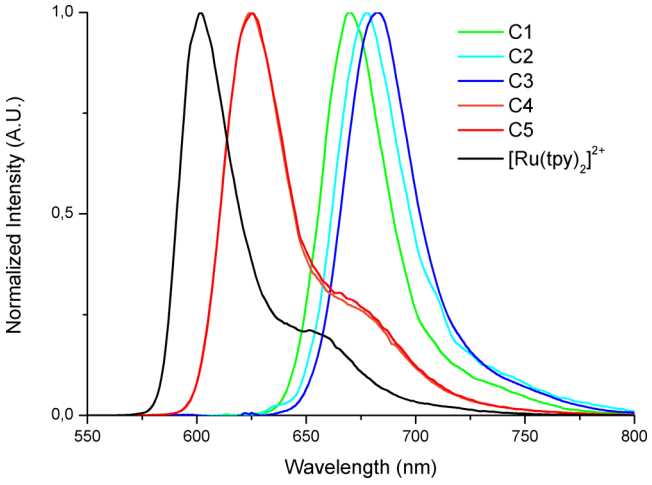

Figure 4. Normalized emission spectra in butyronitrile rigid matrix at 77 K.

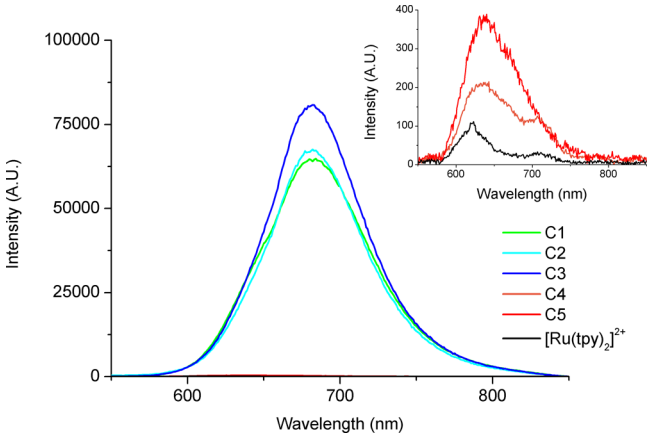

Figure 5. Emission spectra in acetonitrile solution at 298 K, [complex] = 10^{-5} mol L^{-1}. The inset is an expansion of the main graph showing the weak emission of **C4**, **C5**, and $[Ru(tpy)_2]^{2+}$.

three) emission bands, one (or two) for the peripheral Ru(II) centers (similar to the complexes **C4** and **C5**), and one for the central Ru(II) moiety. As a consequence, the presence of only one emission band for complexes **C1**–**C3** suggests some interaction between the Ru(II) centers, which is in agreement with the absorption data.

At room temperature, it is well-known that $[Ru(tpy)_2]^{2+}$ is almost non-luminescent.[5] Complexes **C4**–**C5** are also characterized by a negligible luminescence (Figure 5); a moderate increase of the intensity of this residual emission can still be observed from **C4** to **C5**, as the number of Ru(II) centers increases. Very interestingly, complexes **C1**–**C3** are luminescent at 298 K; the presence of the central Ru(II) center increases the luminescence of the polynuclear complexes by 2 orders of magnitude compared to $[Ru(tpy)_2]^{2+}$, as shown by the quantum yields of emission (Table 2).

Analysis of the Luminescence Profile. A detailed analysis of the shape of the emission spectra at 77K allows more information on the excited-state properties to be obtained by an approach developed by Meyer.[67−71] For all the complexes, a Franck−Condon line-shape analysis using a model with two modes of vibration was used. The results of the fitting of the experimental data are gathered in Table 3; Figure 6 shows the fitting for the complex **C1** (fitting for other

Table 3. Emission Parameters from Franck−Condon Line-Shape Analysis[a]

Complex	E_{00} (cm^{-1})	$\hbar\omega_M$ (cm^{-1})	S_M	$\hbar\omega_L$ (cm^{-1})	S_L	fwhm (cm^{-1})
C1	14960	1220	0.09	530	0.25	670
C2	14690	1240	0.06	590	0.20	700
C3	14800	1320	0.08	590	0.26	680
C4	16120	1190	0.26	400	0.60	610
C5	16140	1190	0.27	380	0.68	600
$[Ru(tpy)_2]^{2+}$	16680	1290	0.23	440	0.56	530

[a]At 77 K in butyronitrile rigid matrix, no parameters were constrained (or fixed) for the fitting calculations.

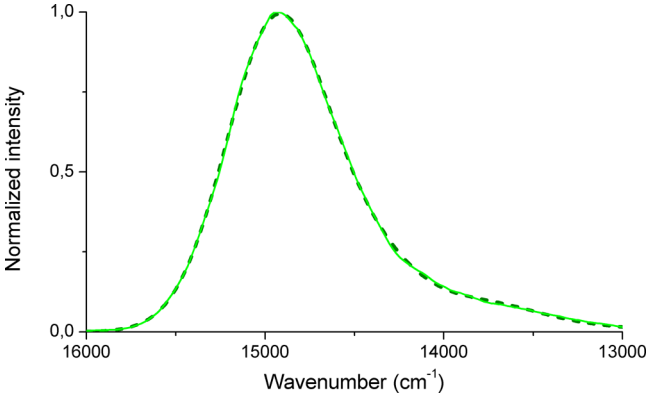

Figure 6. Franck−Condon line-shape analysis of the luminescence spectrum of **C1** at 77 K. The green line is the luminescence **C1**, and the dashed gray line is the fitting.

complexes are presented in Figure S42−S46). The values obtained for the energy of the vibration modes allow distinguishing for each complex a medium frequency vibrational mode ($\hbar\omega_M$) associated with C−C or C−N vibration of the ligand, and a low frequency vibrational mode ($\hbar\omega_L$) corresponding to a metal−ligand bound stretching. These two modes of vibration are associated with Huang−Rhys factors (S_M and S_L), associated with the reorganization energy of the electronic states. E_{00} is the energy of the 0−0 transition, and fwhm is the bandwidth at half-maximum of the vibronic band.

Complexes **C4**–**C5** display a similar behavior to the reference complex $[Ru(tpy)_2]^{2+}$, which is consistent with the assumption that these complexes are only polynuclear assemblies of the reference unit $[Ru(tpy)_2]^{2+}$. For complexes **C1**–**C3** the very low displacement parameter $S_{M/L}$ indicates that the energy curve of the excited state is slightly displaced with respect to the ground state. This was attributed to efficient electron delocalization over the accepting ligand, which induces small changes in the C−C and C−N bond.[72] For complexes **C1**–**C3** the delocalization of the ^{3}MLCT state over the triterpyridine bridging ligand lowers the direct nonradiative deactivation from the ^{3}MLCT excited state to the ground state as previously reported.[72−77]

Luminescence Lifetime. The lifetimes of luminescence of all the complexes at 77 K in a rigid matrix and for the complexes **C1**–**C3** at 298 K are reported in Table 2. In all cases, the luminescence signal decays as a monoexponential. At 77 K, the lifetimes span over 12.0 and 4.8 μs, typical values for Ru(II) complexes with terpyridine ligands.[5] At 298 K only the lifetime of the complexes **C1**–**C3** can be measured due to the

DOI: 10.1021/acs.inorgchem.7b03040
Inorg. Chem. XXXX, XXX, XXX−XXX

low luminescence of the other complexes. Unexpectedly, the lifetimes at 298 K for the complexes **C1**−**C3** are quite long for classical Ru(II) bis-terpyridine complexes; once again, the presence of only one lifetime component for these complexes which have two or three nonchemically equivalent Ru(II) centers indicates that only one of them accounts for the radiative deactivation. The comparison of complexes **C1**−**C3** with complexes **C4**−**C5** suggests that this behavior is induced by the central Ru(II) on the bridging ligands.

In order to gain more information on the deactivation pathways of the excited state, we studied the dependence of luminescence lifetime as a function of temperature (Figure 7);

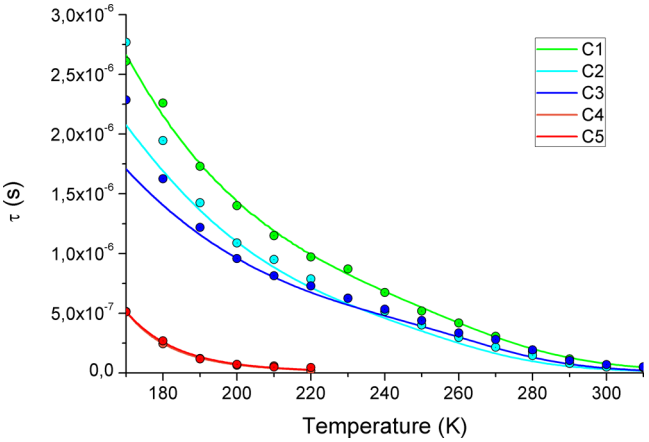

Figure 7. Luminescence lifetime of complexes **C1**−**C5** in butyronitrile as a function of temperature. Data fitted according to the van Houten−Watts equation.[78]

since the seminal work of van Houten and Watts,[78] it is well-known that the variation of luminescence lifetime as a function of the temperature can be interpreted thanks to the following equation:

$$1/\tau = k_r + k_{nr} + \sum A_i e^{[-\Delta E_i/(RT)]} \quad (2)$$

where k_r and k_{nr} are the radiative and vibrational nonradiative rate constants, considered to be constant in the range of temperature studied, and A_i and ΔE_i, the parameters of thermally activated deactivation pathways involved in the decay of the emissive excited state. Such temperature-dependent deactivation can correspond to the shift to another high-energy ^{3}MLCT excited state or a nonemissive ^{3}MC state.

Complexes **C4**−**C5** have a behavior similar to that of the reference complex $[Ru(tpy)_2]^{2+}$. The nonluminescence at 298 K is due to an efficient population of the ^{3}MC state due to the low energy activation ($\Delta E_1 \approx 1600$ cm^{-1}) for the ^{3}MLCT−^{3}MC transition; the nonradiative deactivation from the ^{3}MC state to the ground state is thus the prevailing pathway of deactivation in this case. At lower temperature, thermal access to the ^{3}MC is disfavored and therefore the direct radiative and nonradiative deactivation (k_r and k_{nr}) pathways become dominant, allowing the detection of luminescence of the complexes.

The fittings of the data of complexes **C1**−**C3** require the use of a biexponential expression, meaning that there are at least two thermally activated deactivation pathways accessible for these complexes.[80] This fact is well-known for polypyridyl Ru(II) complexes,[81] and it is due to the presence of upper lying accessible ^{3}MLCT.[72,79−82] In $[Ru(bpy)_3]^{2+}$, the excited ^{3}MLCT state corresponds in fact to a manifold of three undiscernible ^{3}MLCT states and a fourth ^{3}MLCT, which can only be seen at low temperature, localized ≈700 cm^{-1} above the three former ones.[74,81,82] In our case, we can clearly identify a similar pattern for the excited states of complexes **C1**−**C3** (Table 4).

In conclusion, these temperature dependent measurements allowed us to determine that, for complexes **C1**−**C3**, thermally activated relaxation pathways imply: (i) a relaxation through the ^{3}MC state, which correspond to the high energy activation ($\Delta E_1 = E^{\#} \approx 4000$ cm^{-1}) [The A_i factor corresponds to an Arrhenius-type preexponential factor ($A_1 \approx 10^{15}$ s^{-1}) for an irreversible ^{3}MLCT-^{3}MC transition.]; (ii) a population of a high ^{3}MLCT excited state ($\Delta E_2 = \Delta G \approx 700$ cm^{-1}) in equilibrium with the emissive ^{3}MLCT state [In this case, the A_i factor corresponds to the rate constant for the deactivation of this high-energy ^{3}MLCT ($A_1 \approx 10^7$ s^{-1}).] Photophysical schemes for **C1** and **C4** summarizing the deactivation pathways of excited states are depicted in Scheme 3.

Transient-Absorption Spectroscopy. Complexes **C1**−**C3** were studied at room temperature by nanosecond transient absorption spectroscopy (due to the short lifetime of the excited states of **C4**−**C5** and $[Ru(tpy)_2]^{2+}$, they cannot be studied by transient absorption in this time scale). The transient spectra for **C1** (Figure 8) show the bleaching of the ground state around 500 nm, with a lifetime of 95 ns. A positive transient absorption band appearing beyond 600−620 nm and a lifetime of 99 ns are also observed. The lifetimes of these two features are consistent with the luminescence lifetime of the complex (101 ns); a similar behavior was observed for complexes **C2**−**C3** (see Figures S47−S48).

Previous works have shown that for mononuclear Ru(II) terpyridine complexes, a positive transient absorption spectrum can be observed around 600 nm,[83] whereas in the case of polynuclear Ru(II) terpyridine complexes, the transient absorption is red-shifted in the 600−900 nm region;[72,75] these transients have been attributed to the absorption of excited states delocalized over the polyazaaromatic bridging ligand. Our observations are consistent with literature, and we

Table 4. Kinetic Parameters for the Excited-State Decay in Acetonitrile Solution

Complexes	k_0 (s^{-1})	A_1 (s^{-1})	ΔE_1 (cm^{-1})	A_2 (s^{-1})	ΔE_2 (cm^{-1})
C1	1.3×10^5	9.9×10^{14}	3850	6.2×10^7	650
C2	2.6×10^5	1×10^{16}	4200	1.9×10^8	800
C3	2.6×10^5	3.1×10^{16}	4550	7.8×10^7	650
C4	1.1×10^5	1.8×10^{12}	1650		
C5	2.9×10^5	1.6×10^{12}	1650		
$[Ru(tpy)_2]^{2+a}$	1.1×10^5	1.9×10^{13}	1500		

[a]From ref 79.

DOI: 10.1021/acs.inorgchem.7b03040
Inorg. Chem. XXXX, XXX, XXX−XXX

Scheme 3. Photophysical Schemes for Complexes C1 and C4

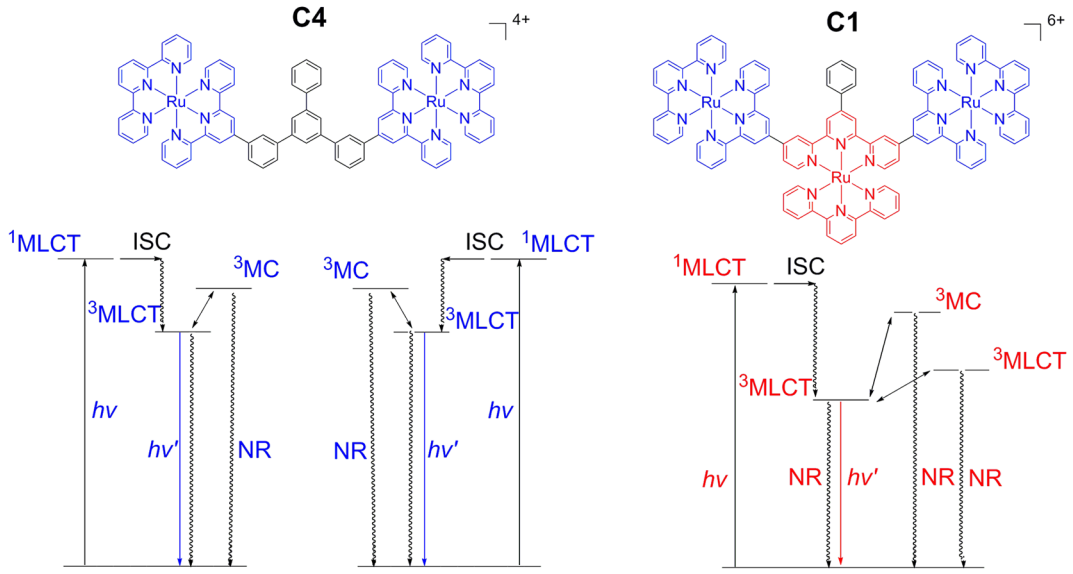

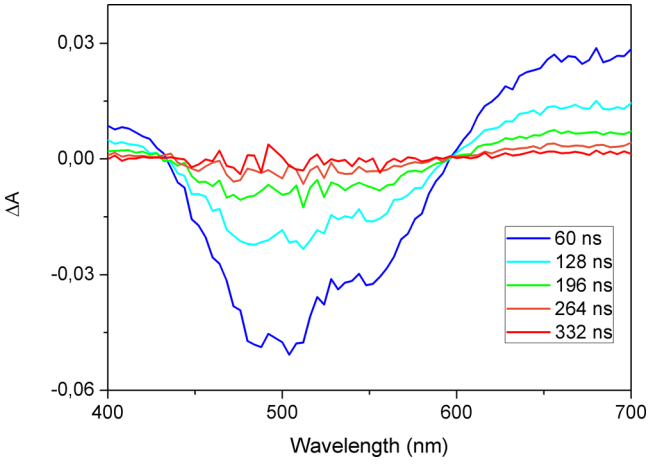

Figure 8. Transient absorption spectra at 298 K of the complex **C1** upon excitation at 355 nm.

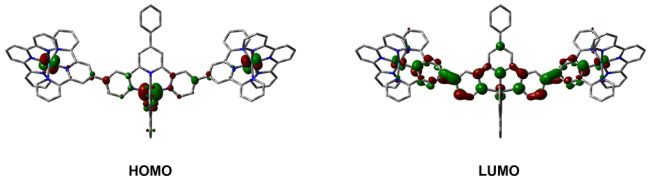

Figure 9. Kohn–Sham electron density illustration of the molecular orbitals of the HOMO and LUMO for **C1** in the (S = 0) ground state.

can safely assert that for **C1–C3**, the ^{3}MLCT excited state is localized over the bridging ligand.

It should be noted that energy transfer processes between the different metallic centers are taking place in the femtosecond time scale and therefore are not observed here.[76,84–86]

Theoretical Calculations. In order to better understand the photophysical behavior of our complexes, theoretical calculations were undertaken on the complex **C1** (Tables S1–S3 and Figures S49–S51). The Kohn–Sham electron density illustrations of the molecular orbitals of the HOMO and the LUMO for the complex **C1** are shown in Figure 9 and Figure S49 in the SI, along with the molecular orbital (MO) contribution tabulated in Table S1 in the SI for the frontiers orbitals.

As expected from the electrochemical and photophysical data, the composition of the HOMO orbital is mostly Ru based (overall 68%) with a minor contribution of the bridging ligand (20%); the LUMO is mostly localized on the main bridging ligand, with a contribution of roughly 89%. Detailed DFT calculations were performed on the first reduced state of the metal complex **C1**; as supposed previously, the first reduced state is also localized on the bridging ligand. The experimental and the theoretical potential for the first reduction are in good agreement (calculated: 3.69 eV, experimental: 3.76 eV).

The simulated absorption spectrum is depicted in Figure S51, and the different contributions are listed in Table S3. The calculations show that the MLCT band is constituted of two different ^{1}MLCT transitions from the different Ru(II) to the bridging ligand, as postulated from the experimental data.

Discussion. Two different behaviors are observed for the five new complexes synthesized. Complexes **C4** and **C5** can be considered as simple polynuclear assemblies of the reference complex $[Ru(tpy)_2]^{2+}$, like other polynuclear complexes reported in the literature.,[32,34,35,37,40–43] with no additional electrochemical or photophysical properties compared to the $[Ru(tpy)]^{2+}$ unit. The situation is very different for complexes **C1–C3**. Indeed, for these complexes, thanks to the inequivalent *central* terpyridine binding site of their constituting ligands **L1–L3** differing from the peripheral ones, novel interesting properties arise in the polynuclear assemblies, which do not correspond to the classic $[Ru(tpy)]^{2+}$.

Antenna Effect. The presence of only one type of emitting level for a polynuclear complex in which nonequivalent chromophores are present suggests the occurrence of an antenna effect. This effect corresponds to an energy transfer process from the peripheral to the central unit. We postulate that complexes **C1–C3** behave according to this principle. Indeed, the UV–visible spectra and the theoretical calculations have shown that the broad absorption band in the visible region implies at least two different MLCT transitions: one from the peripheral Ru(II) to the bridging ligand, and one less energetic from the central Ru(II) to the bridging ligand (Scheme 4). The

DOI: 10.1021/acs.inorgchem.7b03040
Inorg. Chem. XXXX, XXX, XXX–XXX

Scheme 4. Qualitative Energy Diagram and Suggested Mechanism of the Antenna Effect in C1

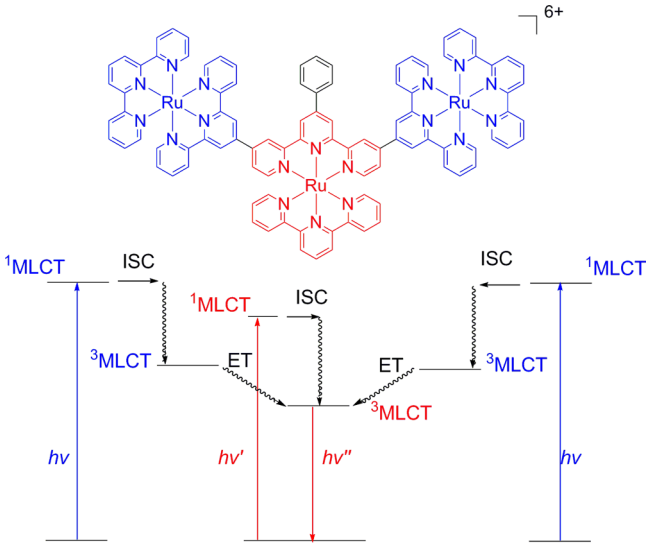

presence of only one emission band with a monoexponential decay, at 77 K as well as 298 K, suggests that emission takes place from a single type of excited state, implying energy transfer processes.

The characteristics of the luminescence of complexes **C1**−**C3**, compared to **C4**−**C5**, where only peripheral Ru(II) units are present, provide information on the direction of the energy transfer taking place within the polynuclear assemblies. At 77 K the bathochromic shift of the emission from **C4**−**C5** to **C1**−**C3** indicates that the peripheral Ru(II) entity is not emissive in the later compounds. The luminescence of **C1**−**C3** at 298 K, in contrast to the nearly nonluminescence of **C4**−**C5**, suggests that in the former compounds it is the central Ru(II) centers which are emissive. The close match between the absorption and the excitation spectra allowed us to rule out the presence of any impurities but also indicates that the energy transfer from the peripheral to the central Ru(II) unit has 100% efficiency,[86] as only one luminescence band is detected. We suggest that the energy transfer takes place through a Dexter mechanism as previously shown for polymetallic antenna.[5] Based on the maxima of luminescence of the complexes **C1**−**C3** and their analogs **C4**−**C5**, we can estimate the driving force for the energy transfer from peripheral to central Ru(II) to be approximately −0.12 eV at 298 K. In the case of **C1**, the two equivalent peripheral Ru(II) centers transfer their energy to the emissive central Ru(II) center. Among the three peripheral Ru(II) centers of **C2**, two are chemically equivalent. Along the same train of thought, it is likely that the three peripheral Ru(II) centers transfer their energy to the central Ru(II) moiety (see Figure S52). Indeed, the similarity of the emission profiles between **C2** and **C1** supports this assumption (Figures 4 and 5). The behavior of **C3**, which can be seen as the assembly of two **C1** subunits, is similar to that of **C1**; energy transfer is taking place from the peripheral Ru(II) centers to the two equivalent central Ru(II) centers (see Figure S53). The fact that the photophysical properties of **C1** and **C3** are quasi identical confirms the absence of interaction between the two emissive central metallic moieties.[87]

Excited-State Properties. Very interestingly, the luminescence lifetime and quantum yield of complexes **C1**−**C3** are quite long and high, respectively, for Ru(II) terpyridine complexes in contrast to **C4**−**C5**, which have properties similar to $[Ru(tpy)_2]^{2+}$. The electrochemical analysis of complexes **C1**−**C3** shows the presence of a new reduction wave at higher potential than for **C4**−**C5** and $[Ru(tpy)_2]^{2+}$, assigned to the reduction of the central bridging ligand; in agreement with theoretical calculations, we suggest that the LUMO is thus localized over the central tpy ligand for these complexes. In contrast, for all the complexes, the oxidation of Ru(II) arises at similar potentials, and therefore, the HOMO is supposed to be localized on the Ru(II) centers, which are equivalent. In the excited state, the transient absorption shows the reduction of the bridging ligand and the bleaching at 500 nm suggests an oxidation of the Ru(II) to Ru(III) for **C1**−**C3**. The correspondence between the lifetimes of the two processes suggests that the lowest-lying excited state is a metal-to-ligand charge-transfer transition from the central Ru(II) center to the bridging ligand.

Analysis of the luminescence profile shows that the excited state for **C1**−**C3** is strongly delocalized over the bridging ligand. The evolution of the luminescent lifetime with temperature allows us to have a better insight into the photophysics of our complexes. In the case of **C4**−**C5**, like for $[Ru(tpy)_2]^{2+}$, the main deactivation pathway of the excited ^{3}MLCT state is the thermal population of a nonluminescent ^{3}MC state, making these complexes almost nonluminescent at room temperature. For complexes **C1**-**C3**, the stabilization of the LUMO localized over the central ligand lowers the energy of the ^{3}MLCT state, hence increasing the activation energy required for the ^{3}MLCT-^{3}MC transition; i.e. from approximately 1600 cm^{-1} for **C4**−**C5** to 4000 cm^{-1} for **C1**−**C3**. As a consequence, the thermal population of the ^{3}MC state is less efficient, allowing the ^{3}MLCT state to deactivate radiatively. We were also able to evidence the equilibrium with another ^{3}MLCT state in this case. The different information gathered in this study allowed us to suggest a photophysical scheme presented in Scheme 4 for complex **C1**. Similar photophysical schemes are suggested for complexes **C2** and **C3** (presented in SI, Figures S52−S53).

CONCLUSIONS

The complexes **C1**−**C3** combine two interesting properties: an antenna effect and a delocalization of the excited state. By an adequate design of the bridging ligand an efficient convergent energy transfer from the peripheral to the central Ru(II) center with a driving force of −0.12 eV is induced. Afterward the delocalization of the ^{3}MLCT excited state of the energy acceptor results in a substantial increase of the luminescence lifetime and quantum yield by 2 orders of magnitude in comparison with the reference complex $[Ru(tpy)_2]^{2+}$. The result of the synergetic combination of both effects is the formation of a polymetallic molecular antenna made of terpyridine Ru(II) complexes with improved photophysical properties. The comparison of the complexes **C1** and **C3** with their analog complexes **C4**−**C5** without the central Ru(II) center confirms of the importance of the latter for the improvement of the photophysical properties. For the five complexes, the main pathway of deactivation at 298 K is the thermal population of the ^{3}MC; the electron delocalization in complexes **C1**−**C3** increases the energy barrier for the thermal population of ^{3}MC, hence increasing the radiative deactivation. The benefical effect of the delocalization of the excited state in binuclear Ru(II) terpyridine complexes was previously under-

DOI: 10.1021/acs.inorgchem.7b03040
Inorg. Chem. XXXX, XXX, XXX−XXX

lined by Sauvage and co-workers.[72] Although, to the best of our knowledge, it is the first time that the delocalization of the excited state is combined with an antenna effect for polynuclear Ru(II) terpyridine complexes. As a consequence, complexes **C1**−**C3** are promising building blocks to connect to a final acceptor or a catalytic center.

■ ASSOCIATED CONTENT

Supporting Information

The Supporting Information is available free of charge on the ACS Publications website at DOI: 10.1021/acs.inorgchem.7b03040.

^{1}H NMR spectra, ^{13}C NMR spectra, mass spectra, cyclic voltammograms, excitation spectra, transient absorption spectra, and theoretical calculations (PDF)

■ AUTHOR INFORMATION

Corresponding Author

*E-mail: Benjamin.Elias@uclouvain.be.

ORCID

Simon Cerfontaine: 0000-0002-9865-762X

Lionel Marcélis: 0000-0002-6324-477X

Garry S. Hanan: 0000-0001-6671-5234

Notes

The authors declare no competing financial interest.

■ ACKNOWLEDGMENTS

S.C., L.M., and B.E. gratefully acknowledge the Université catholique de Louvain, the "Fonds National pour la Recherche Scientifique (FRS-FNRS)", the Région Wallonne, and the Fondation Louvain (Prix Pierre et Colette Bauchau) for financial support. G.S.H. and B.L.-M. thank the Natural Sciences and Engineering Research Council (NSERC) of Canada. B.E. and G.S.H. thank the Québec-Wallonie program for financial support. F.L. thanks the ICMG Chemistry Nanobio Platform for technical support. The UMONS MS laboratory acknowledges the "Fonds National pour la Recherche Scientifique (FRS-FNRS)" for its contribution to the acquisition of the Waters QToF Premier and the Synapt G2-S*i* mass spectrometer and for continuing support.

■ REFERENCES

(1) Morgan, G.; Burstall, F. H. Researches on residual affinity and co-ordination. Part XXXVII. Complex metallic salts containing 2:6-di-2′-pyridylpyridine (2:2′: 2″-tripyridyl). *J. Chem. Soc.* **1937**, *0*, 1649−1655.

(2) Burstall, F. H. Optical activity dependent on co-ordinated bivalent ruthenium. *J. Chem. Soc.* **1936**, 173.

(3) Paris, J. P.; Brandt, W. W. Charge Transfer Luminescence of a Ruthenium(II) Chelate. *J. Am. Chem. Soc.* **1959**, *81*, 5001−5002.

(4) Fink, D. W.; Ohnesorge, W. E. Temperature effects on charge-transfer luminescence intensity of some transition metal ion chelates. *J. Am. Chem. Soc.* **1969**, *91*, 4995−4998.

(5) Sauvage, J. P.; Collin, J. P.; Chambron, J. C.; Guillerez, S.; Coudret, C.; Balzani, V.; Barigelletti, F.; De Cola, L.; Flamigni, L. Ruthenium(II) and Osmium(II) Bis(terpyridine) Complexes in Covalently-Linked Multicomponent Systems: Synthesis, Electrochemical Behavior, Absorption Spectra, and Photochemical and Photophysical Properties. *Chem. Rev.* **1994**, *94*, 993−1019.

(6) Juris, A.; Balzani, V.; Barigelletti, F.; Campagna, S.; Belser, P.; von Zelewsky, A. Ru(II) polypyridine complexes: photophysics, photochemistry, eletrochemistry, and chemiluminescence. *Coord. Chem. Rev.* **1988**, *84*, 85−277.

(7) Medlycott, E. A.; Hanan, G. S. Designing tridentate ligands for ruthenium(ii) complexes with prolonged room temperature luminescence lifetimes. *Chem. Soc. Rev.* **2005**, *34*, 133−142.

(8) Tucker, J. W.; Stephenson, C. R. J. Shining Light on Photoredox Catalysis: Theory and Synthetic Applications. *J. Org. Chem.* **2012**, *77*, 1617−1622.

(9) Wei, H.; Wang, E. Electrochemiluminescence of tris(2,2′-bipyridyl)ruthenium and its applications in bioanalysis: a review. *Luminescence* **2011**, *26*, 77−85.

(10) Steed, J. W.; Atwood, J. L. In *Supramol. Chem.*; John Wiley & Sons, Ltd: 2009; pp 707−775.

(11) Marcaccio, M.; Paolucci, F.; Paradisi, C.; Roffia, S.; Fontanesi, C.; Yellowlees, L. J.; Serroni, S.; Campagna, S.; Denti, G.; Balzani, V. Electrochemistry of Multicomponent Systems. Redox Series Comprising up to 26 Reversible Reduction Processes in Polynuclear Ruthenium(II) Bipyridine-Type Complexes. *J. Am. Chem. Soc.* **1999**, *121*, 10081−10091.

(12) Denti, G.; Campagna, S.; Serroni, S.; Ciano, M.; Balzani, V. Decanuclear homo- and heterometallic polypyridine complexes: syntheses, absorption spectra, luminescence, electrochemical oxidation, and intercomponent energy transfer. *J. Am. Chem. Soc.* **1992**, *114*, 2944−2950.

(13) Denti, G.; Serroni, S.; Campagna, S.; Ricevuto, V.; Balzani, V. Made-to-order control of the direction of electronic energy transfer in tetranuclear luminescent metal complexes. *Coord. Chem. Rev.* **1991**, *111*, 227−236.

(14) Campagna, S.; Denti, G.; Serroni, S.; Juris, A.; Venturi, M.; Ricevuto, V.; Balzani, V. Dendrimers of Nanometer Size Based on Metal Complexes: Luminescent and Redox-Active Polynuclear Metal Complexes Containing up to Twenty-Two Metal Centers. *Chem. - Eur. J.* **1995**, *1*, 211−221.

(15) Pal, A. K.; Hanan, G. S. Design, synthesis and excited-state properties of mononuclear Ru(ii) complexes of tridentate heterocyclic ligands. *Chem. Soc. Rev.* **2014**, *43*, 6184−6197.

(16) Hammarström, L.; Johansson, O. Expanded bite angles in tridentate ligands. Improving the photophysical properties in bistridentate RuII polypyridine complexes. *Coord. Chem. Rev.* **2010**, *254*, 2546−2559.

(17) Jäger, M.; Kumar, R. J.; Görls, H.; Bergquist, J.; Johansson, O. Facile Synthesis of Bistridentate RuII Complexes Based on 2,6-Di(quinolin-8-yl)pyridyl Ligands: Sensitizers with Microsecond 3MLCT Excited State Lifetimes. *Inorg. Chem.* **2009**, *48*, 3228−3238.

(18) Breivogel, A.; Förster, C.; Heinze, K. A Heteroleptic Bis(tridentate)ruthenium(II) Polypyridine Complex with Improved Photophysical Properties and Integrated Functionalizability. *Inorg. Chem.* **2010**, *49*, 7052−7056.

(19) Breivogel, A.; Meister, M.; Förster, C.; Laquai, F.; Heinze, K. Excited State Tuning of Bis(tridentate) Ruthenium(II) Polypyridine Chromophores by Push−Pull Effects and Bite Angle Optimization: A Comprehensive Experimental and Theoretical Study. *Chem. - Eur. J.* **2013**, *19*, 13745−13760.

(20) Kreitner, C.; Erdmann, E.; Seidel, W. W.; Heinze, K. Understanding the Excited State Behavior of Cyclometalated Bis-(tridentate)ruthenium(II) Complexes: A Combined Experimental and Theoretical Study. *Inorg. Chem.* **2015**, *54*, 11088−11104.

(21) Bomben, P. G.; Robson, K. C. D.; Koivisto, B. D.; Berlinguette, C. P. Cyclometalated ruthenium chromophores for the dye-sensitized solar cell. *Coord. Chem. Rev.* **2012**, *256*, 1438−1450.

(22) Bonnefous, C.; Chouai, A.; Thummel, R. P. Cyclometalated Complexes of Ru(II) with 2-Aryl Derivatives of Quinoline and 1,10-Phenanthroline. *Inorg. Chem.* **2001**, *40*, 5851−5859.

(23) Brown, D. G.; Sanguantrakun, N.; Schulze, B.; Schubert, U. S.; Berlinguette, C. P. Bis(tridentate) Ruthenium−Terpyridine Complexes Featuring Microsecond Excited-State Lifetimes. *J. Am. Chem. Soc.* **2012**, *134*, 12354−12357.

(24) Pal, A. K.; Zaccheroni, N.; Campagna, S.; Hanan, G. S. Near infra-red emission from a mer-Ru(ii) complex: consequences of strong [sigma]-donation from a neutral, flexible ligand with dual binding modes. *Chem. Commun.* **2014**, *50*, 6846−6849.

DOI: 10.1021/acs.inorgchem.7b03040
Inorg. Chem. XXXX, XXX, XXX−XXX

(25) Pal, A. K.; Serroni, S.; Zaccheroni, N.; Campagna, S.; Hanan, G. S. Near infra-red emitting Ru(ii) complexes of tridentate ligands: electrochemical and photophysical consequences of a strong donor ligand with large bite angles. *Chem. Sci.* **2014**, *5*, 4800−4811.
(26) Laramee-Milette, B.; Hanan, G. S. Ruthenium bistridentate complexes with non-symmetrical hexahydro-pyrimidopyrimidine ligands: a structural and theoretical investigation of their optical and electrochemical properties. *Dalton Trans.* **2016**, *45*, 12507−12517.
(27) Constable, E. C.; Housecroft, C. E.; Thompson, A. C.; Passaniti, P.; Silvi, S.; Maestri, M.; Credi, A. pH-sensitive Ru(II) and Os(II) bis(2,2′:6′,2″-terpyridine) complexes: A photophysical investigation. *Inorg. Chim. Acta* **2007**, *360*, 1102−1110.
(28) Maestri, M.; Armaroli, N.; Balzani, V.; Constable, E. C.; Thompson, A. M. W. C. Complexes of the Ruthenium(II)-2,2′:6′,2″-terpyridine Family. Effect of Electron-Accepting and -Donating Substituents on the Photophysical and Electrochemical Properties. *Inorg. Chem.* **1995**, *34*, 2759−2767.
(29) Nastasi, F.; Loiseau, F.; Campagna, S.; Medlycott, E. A.; Santoni, M.-P.; Hanan, G. S. Synthesis and photophysical properties of naphthyl-, phenanthryl-, and pyrenyl-appended bis(pyridyl)triazine ligands and their Zn(II) and Ru(II) complexes1. *Can. J. Chem.* **2009**, *87*, 254−263.
(30) Rousset, E.; Chartrand, D.; Ciofini, I.; Marvaud, V.; Hanan, G. S. Red-light-driven photocatalytic hydrogen evolution using a ruthenium quaterpyridine complex. *Chem. Commun.* **2015**, *51*, 9261−9264.
(31) Laramee-Milette, B.; Nastasi, F.; Puntoriero, F.; Campagna, S.; Hanan, G. S. Photo-Induced Assembly of a Luminescent Tetraruthenium Square. *Chem. - Eur. J.* **2017**, *23*, 16497−16504.
(32) Constable, E. C.; Thompson, A. M. W. C. A new ligand for the self assembly of starburst coordination oligomers and polymers. *J. Chem. Soc., Chem. Commun.* **1992**, 617−619.
(33) Arana, C. R.; Abruna, H. D. Monomeric and oligomeric complexes of ruthenium and osmium with tetra-2-pyridyl-1,4-pyrazine (TPPZ). *Inorg. Chem.* **1993**, *32*, 194−203.
(34) Newkome, G. R.; Cardullo, F.; Constable, E. C.; Moorefield, C. N.; Thompson, A. M. W. C. Metallomicellanols: incorporation of ruthenium(II)-2,2′: 6′,2″-terpyridine triads into cascade polymers. *J. Chem. Soc., Chem. Commun.* **1993**, *0*, 925−927.
(35) Hanan, G. S.; Arana, C. R.; Lehn, J.-M.; Fenske, D. Synthesis, Structure, and Properties of Dinuclear and Trinuclear Rack-Type RuII Complexes. *Angew. Chem., Int. Ed. Engl.* **1995**, *34*, 1122−1124.
(36) Hanan, G. S.; Arana, C. R.; Lehn, J.-M.; Baum, G.; Fenske, D. Coordination Arrays: Synthesis and Characterisation of Rack-Type Dinuclear Complexes. *Chem. - Eur. J.* **1996**, *2*, 1292−1302.
(37) Ceroni, P.; Credi, A.; Balzani, V.; Campagna, S.; Hanan, G. S.; Arana, C. R.; Lehn, J.-M. Absorption and Emission Properties of Di- and Trinuclear Ruthenium(II) Rack-Type Complexes. *Eur. J. Inorg. Chem.* **1999**, *1999*, 1409−1414.
(38) Newkome, G. R.; Cho, T. J.; Moorefield, C. N.; Cush, R.; Russo, P. S.; Godínez, L. A.; Saunders, M. J.; Mohapatra, P. Hexagonal Terpyridine−Ruthenium and − Iron Macrocyclic Complexes by Stepwise and Self-Assembly Procedures. *Chem. - Eur. J.* **2002**, *8*, 2946−2954.
(39) Vaduvescu, S.; Potvin; Pierre, G. Linear Multinuclear RuII Photosensitizers. *Eur. J. Inorg. Chem.* **2004**, *2004*, 1763−1769.
(40) Cavazzini, M.; Quici, S.; Scalera, C.; Puntoriero, F.; La Ganga, G.; Campagna, S. Synthesis, Characterization, Absorption Spectra, and Luminescence Properties of Multinuclear Species Made of Ru(II) and Ir(III) Chromophores. *Inorg. Chem.* **2009**, *48*, 8578−8592.
(41) Yuan, J.; Jiang, Z.; Liu, D.; Li, Y.; Wang, P. Synthesis and photophysical properties of multi-Ru2+ terpyridine complexes: from di-nuclear linear to star-shaped hexa-nuclear architectures. *Inorg. Chem. Front.* **2016**, *3*, 268−273.
(42) Liu, D.; Jiang, Z.; Wang, M.; Yang, X.; Liu, H.; Wu, T.; Wang, P. Highly packed and stretched polyterpyridinyl Ru2+ complexes and their photophysical and stability properties. *Inorg. Chim. Acta* **2016**, *450*, 293−298.
(43) Yan, W.; Réthoré, C.; Menning, S.; Brenner-Weiß, G.; Muller, T.; Pierrat, P.; Bräse, S. A Hexakis Terpyridine-Fullerene Ligand in Six-Fold Ruthenium, Iridium, and Iron Complexes: Synthesis and Electrochemical Properties. *Chem. - Eur. J.* **2016**, *22*, 11522−11526.
(44) Hasenknopf, B.; Hall, J.; Lehn, J. M.; Balzani, V.; Credi, A.; Campagna, S. Linear tris-terpyridines and their trinuclear Ru(ll) complexes: Synthesis, absorption spectra, and excited state properties. *New J. Chem.* **1996**, *20*, 725−730.
(45) Jacques, A.; Cerfontaine, S.; Elias, B. Access to Functionalized Luminescent Multi-2,2′:6′,2″-terpyridine Ligands. *J. Org. Chem.* **2015**, *80*, 11143−11148.
(46) Adamski-Werner, S. L.; Palaninathan, S. K.; Sacchettini, J. C.; Kelly, J. W. Diflunisal Analogues Stabilize the Native State of Transthyretin. Potent Inhibition of Amyloidogenesis. *J. Med. Chem.* **2004**, *47*, 355−374.
(47) Xie, T. Z.; Liao, S. Y.; Guo, K.; Lu, X.; Dong, X.; Huang, M.; Moorefield, C. N.; Cheng, S. Z.; Liu, X.; Wesdemiotis, C.; Newkome, G. R. Construction of a highly symmetric nanosphere via a one-pot reaction of a tristerpyridine ligand with Ru(II). *J. Am. Chem. Soc.* **2014**, *136*, 8165−8.
(48) Frisch, M. J.; Trucks, G. W.; Schlegel, H. B.; Scuseria, G. E.; Robb, M. A.; Cheeseman, J. R.; Scalmani, G.; Barone, V.; Mennucci, B.; Petersson, G. A.; Nakatsuji, H.; Caricato, M.; Li, X.; Hratchian, H. P.; Izmaylov, A. F.; Bloino, J.; Zheng, G.; Sonnenberg, J. L.; Hada, M.; Ehara, M.; Toyota, K.; Fukuda, R.; Hasegawa, J.; Ishida, M.; Nakajima, T.; Honda, Y.; Kitao, O.; Nakai, H.; Vreven, T.; Montgomery, J. A., Jr.; Peralta, J. E.; Ogliaro, F.; Bearpark, M. J.; Heyd, J. J.; Brothers, E. N.; Kudin, K. N.; Staroverov, V. N.; Kobayashi, R.; Normand, J.; Raghavachari, K.; Rendell, A. P.; Burant, J. C.; Iyengar, S. S.; Tomasi, J.; Cossi, M.; Rega, N.; Millam, J. M.; Klene, M.; Knox, J. E.; Cross, J. B.; Bakken, V.; Adamo, C.; Jaramillo, J.; Gomperts, R.; Stratmann, R. E.; Yazyev, O.; Austin, A. J.; Cammi, R.; Pomelli, C.; Ochterski, J. W.; Martin, R. L.; Morokuma, K.; Zakrzewski, V. G.; Voth, G. A.; Salvador, P.; Dannenberg, J. J.; Dapprich, S.; Daniels, A. D.; Farkas, O.; Foresman, J. B.; Ortiz, J. V.; Cioslowski, J.; Fox, D. J. *Gaussian 09*, revision E.01; Gaussian, Inc.: Wallingford, CT, 2009.
(49) Miehlich, B.; Savin, A.; Stoll, H.; Preuss, H. Results obtained with the correlation energy density functionals of becke and Lee, Yang and Parr. *Chem. Phys. Lett.* **1989**, *157*, 200−206.
(50) Becke, A. D. Density-functional thermochemistry. III. The role of exact exchange. *J. Chem. Phys.* **1993**, *98*, 5648−5652.
(51) Lee, C.; Yang, W.; Parr, R. G. Development of the Colle-Salvetti correlation-energy formula into a functional of the electron density. *Phys. Rev. B: Condens. Matter Mater. Phys.* **1988**, *37*, 785−789.
(52) Stevens, W. J.; Krauss, M.; Basch, H.; Jasien, P. G. Relativistic compact effective potentials and efficient, shared-exponent basis sets for the third-, fourth-, and fifth-row atoms. *Can. J. Chem.* **1992**, *70*, 612−630.
(53) Cundari, T. R.; Stevens, W. J. Effective core potential methods for the lanthanides. *J. Chem. Phys.* **1993**, *98*, 5555−5565.
(54) Stevens, W. J.; Basch, H.; Krauss, M. Compact effective potentials and efficient shared-exponent basis sets for the first- and second-row atoms. *J. Chem. Phys.* **1984**, *81*, 6026−6033.
(55) Binkley, J. S.; Pople, J. A.; Hehre, W. J. Self-consistent molecular orbital methods. 21. Small split-valence basis sets for first-row elements. *J. Am. Chem. Soc.* **1980**, *102*, 939−947.
(56) Dennington, R.; Keith, J. A.; Millam, J. M. *GaussView*, version 5.0.9; Gaussian Inc.: Shawnee Mission, KS, 2009.
(57) O'Boyle, N. M.; Tenderholt, A. L.; Langner, K. M. cclib: A library for package-independent computational chemistry algorithms. *J. Comput. Chem.* **2008**, *29*, 839−845.
(58) Skripnikov, L. *Chemissian*, version 4.30; Chemissian, 2005−2016.
(59) Miertuš, S.; Scrocco, E.; Tomasi, J. Electrostatic interaction of a solute with a continuum. A direct utilizaion of AB initio molecular potentials for the prevision of solvent effects. *Chem. Phys.* **1981**, *55*, 117−129.
(60) Tomasi, J.; Mennucci, B.; Cammi, R. Quantum Mechanical Continuum Solvation Models. *Chem. Rev.* **2005**, *105*, 2999−3094.
(61) Aspley, C. J.; Gareth Williams, J. A. Palladium-catalysed cross-coupling reactions of ruthenium bis-terpyridyl complexes: strategies

DOI: 10.1021/acs.inorgchem.7b03040
Inorg. Chem. XXXX, XXX, XXX−XXX

for the incorporation and exploitation of boronic acid functionality. *New J. Chem.* **2001**, *25*, 1136−1147.
(62) Sullivan, B. P.; Calvert, J. M.; Meyer, T. J. Cis-trans isomerism in (trpy)(PPh3)RuC12. Comparisons between the chemical and physical properties of a cis-trans isomeric pair. *Inorg. Chem.* **1980**, *19*, 1404−1407.
(63) Constable, E. C.; Thompson, A. M. W. C. Multinucleating 2,2[prime or minute]: 6[prime or minute],2[double prime]-terpyridine ligands as building blocks for the assembly of co-ordination polymers and oligomers. *J. Chem. Soc., Dalton Trans.* **1992**, 3467−3475.
(64) Karas, M.; Glückmann, M.; Schäfer, J. Ionization in matrix-assisted laser desorption/ionization: singly charged molecular ions are the lucky survivors. *J. Mass Spectrom.* **2000**, *35*, 1−12.
(65) Campagna, S.; Serroni, S.; Bodige, S.; MacDonnell, F. M. Absorption Spectra, Photophysical Properties, and Redox Behavior of Stereochemically Pure Dendritic Ruthenium(II) Tetramers and Related Dinuclear and Mononuclear Complexes. *Inorg. Chem.* **1999**, *38*, 692−701.
(66) Balzani, V.; Juris, A.; Venturi, M.; Campagna, S.; Serroni, S. Luminescent and Redox-Active Polynuclear Transition Metal Complexes. *Chem. Rev.* **1996**, *96*, 759−834.
(67) Caspar, J. V.; Meyer, T. J. Photochemistry of MLCT excited states. Effect of nonchromophoric ligand variations on photophysical properties in the series cis-Ru(bpy)2L22+. *Inorg. Chem.* **1983**, *22*, 2444−2453.
(68) Caspar, J. V.; Meyer, T. J. Photochemistry of tris(2,2′-bipyridine)ruthenium(2+) ion (Ru(bpy)32+). Solvent effects. *J. Am. Chem. Soc.* **1983**, *105*, 5583−5590.
(69) Allen, G. H.; White, R. P.; Rillema, D. P.; Meyer, T. J. Synthetic control of excited-state properties. Tris-chelate complexes containing the ligands 2,2′-bipyrazine, 2,2′-bipyridine, and 2,2′-bipyrimidine. *J. Am. Chem. Soc.* **1984**, *106*, 2613−2620.
(70) Caspar, J. V.; Westmoreland, T. D.; Allen, G. H.; Bradley, P. G.; Meyer, T. J.; Woodruff, W. H. Molecular and electronic structure in the metal-to-ligand charge-transfer excited states of d6 transition-metal complexes in solution. *J. Am. Chem. Soc.* **1984**, *106*, 3492−3500.
(71) Kober, E. M.; Caspar, J. V.; Lumpkin, R. S.; Meyer, T. J. Application of the energy gap law to excited-state decay of osmium(II)-polypyridine complexes: calculation of relative nonradiative decay rates from emission spectral profiles. *J. Phys. Chem.* **1986**, *90*, 3722−3734.
(72) Hammarström, L.; Barigelletti, F.; Flamigni, L.; Indelli, M. T.; Armaroli, N.; Calogero, G.; Guardigli, M.; Sour, A.; Collin, J.-P.; Sauvage, J.-P. A Study on Delocalization of MLCT Excited States by Rigid Bridging Ligands in Homometallic Dinuclear Complexes of Ruthenium(II). *J. Phys. Chem. A* **1997**, *101*, 9061−9069.
(73) Boyde, S.; Strouse, G. F.; Jones, W. E.; Meyer, T. J. The effect on MLCT excited states of electronic delocalization in the acceptor ligand. *J. Am. Chem. Soc.* **1990**, *112*, 7395−7396.
(74) Coe, B. J.; Thompson, D. W.; Culbertson, C. T.; Schoonover, J. R.; Meyer, T. J. Synthesis and Photophysical Properties of Mono-(2,2′,2″-terpyridine) Complexes of Ruthenium(II). *Inorg. Chem.* **1995**, *34*, 3385−3395.
(75) Liang, Y. Y.; Baba, A. I.; Kim, W. Y.; Atherton, S. J.; Schmehl, R. H. Intramolecular Exchange Energy Transfer in a Bridged Bimetallic Transition Metal Complex: Calculation of Rate Constants Using Emission Spectral Fitting Parameters. *J. Phys. Chem.* **1996**, *100*, 18408−18414.
(76) Larsen, J.; Puntoriero, F.; Pascher, T.; McClenaghan, N.; Campagna, S.; Åkesson, E.; Sundström, V. Extending the Light-Harvesting Properties of Transition-Metal Dendrimers. *ChemPhysChem* **2007**, *8*, 2643−2651.
(77) Damrauer, N. H.; Boussie, T. R.; Devenney, M.; McCusker, J. K. Effects of Intraligand Electron Delocalization, Steric Tuning, and Excited-State Vibronic Coupling on the Photophysics of Aryl-Substituted Bipyridyl Complexes of Ru(II). *J. Am. Chem. Soc.* **1997**, *119*, 8253−8268.
(78) Van Houten, J.; Watts, R. J. Photochemistry of tris(2,2′-bipyridyl)ruthenium(II) in aqueous solutions. *Inorg. Chem.* **1978**, *17*, 3381−3385.
(79) Hecker, C. R.; Gushurst, A. K. I.; McMillin, D. R. Phenyl substituents and excited-state lifetimes in ruthenium(II) terpyridyls. *Inorg. Chem.* **1991**, *30*, 538−541.
(80) Forster, L. S. Thermal relaxation in excited electronic states of d3 and d6 metal complexes. *Coord. Chem. Rev.* **2002**, *227*, 59−92.
(81) Sykora, M.; Kincaid, J. R. Synthetic Manipulation of Excited State Decay Pathways in a Series of Ruthenium(II) Complexes Containing Bipyrazine and Substituted Bipyridine Ligands. *Inorg. Chem.* **1995**, *34*, 5852−5856.
(82) Lumpkin, R. S.; Kober, E. M.; Worl, L. A.; Murtaza, Z.; Meyer, T. J. Metal-to-ligand charge-transfer (MLCT) photochemistry: experimental evidence for the participation of a higher lying MLCT state in polypyridyl complexes of ruthenium(II) and osmium(II). *J. Phys. Chem.* **1990**, *94*, 239−243.
(83) Amouyal, E.; Bahout, M.; Calzaferri, G. Excited states of M(II,d6)-4′-phenylterpyridine complexes: electron localization. *J. Phys. Chem.* **1991**, *95*, 7641−7649.
(84) Andersson, J.; Puntoriero, F.; Serroni, S.; Yartsev, A.; Pascher, T.; Polívka, T.; Campagna, S.; Sundström, V. Ultrafast singlet energy transfer competes with intersystem crossing in a multi-center transition metal polypyridine complex. *Chem. Phys. Lett.* **2004**, *386*, 336−341.
(85) Andersson, J.; Puntoriero, F.; Serroni, S.; Yartsev, A.; Pascher, T.; Polivka, T.; Campagna, S.; Sundstrom, V. New paradigm of transition metal polypyridine complex photochemistry. *Faraday Discuss.* **2004**, *127*, 295−305.
(86) La Mazza, E.; Puntoriero, F.; Nastasi, F.; Laramee-Milette, B.; Hanan, G. S.; Campagna, S. A heptanuclear light-harvesting metal-based antenna dendrimer with six Ru(ii)-based chromophores directly powering a single Os(ii)-based energy trap. *Dalton Trans.* **2016**, *45*, 19238−19241.
(87) To rule out any T-T annihilation, i.e. no interaction between the central Ru(II) centers, the emission intensity was monitored as a function of the power of the excitation source. No decrease of the emission was observed upon increased energy, confirming the absence of T-T annihilation.

DOI: 10.1021/acs.inorgchem.7b03040
Inorg. Chem. XXXX, XXX, XXX−XXX